IN VIVO STUDIES OF ASC SPECKS AS ANTIGEN DELIVERY VEHICLES

by

Seda Yaşa

B.S., Molecular Biology and Genetics, Boğaziçi University, 2014

Submitted to the Institute for Graduate Studies in
Science and Engineering in partial fulfillment of
the requirements for the degree of
Master of Science

Graduate Program in Molecular Biology and Genetics
Boğaziçi University

2016

IN VIVO STUDIES OF ASC SPECKS AS ANTIGEN DELIVERY VEHICLES

APPROVED BY:

Prof. Nesrin Özören (Thesis Supervisor)	.....
Prof. Batu Erman	.....
Assist. Prof. Umut Şahin	.....

DATE OF APPROVAL: 26/08/2016

ACKNOWLEDGEMENTS

First and foremost I offer my sincerest gratitude to my supervisor, Prof. Nesrin Özören, for always being accessible when I needed and her endless support and guidance throughout my thesis and studies. Her friendly and visionary approach generated a great environment to work in and be productive. Additionally, I am grateful to Prof. Batu Erman for his experimental and theoretical mentorship and taking time to evaluate my thesis work. I also would like to thank to my third jury member Assist. Prof. Umut Şahin for devoting his time to evaluate my thesis.

Another scientist to whom I particularly want to thank is Assoc. Prof. Stefan H. Fuss. He was always lending a hand to me when I needed assistance in confocal analysis.

My lab members Aybüke Garipcan, M.Sc., Hulusi Onur Kuzucu, B.Sc., Açelya Yılmazer, B.Sc., Mesut Berber B.Sc. and former lab members Elif Eren, Ph.D., Mustafa Yalçınkaya, B.Sc., Ceren Saygı, M.Sc., Serkan Uğurlu, M.D.-Ph.D. were always available when I needed any help. I am grateful for their collaboration and sincere friendship. Also, I would like to thank Zeynep Karagöz B.Sc. for her works on ASC specks as a special project student.

Furthermore, I would like to thank the hard-working people working in Vivarium of Boğaziçi University. Especially to D.V.M. Arzu Temizyürek, Leyla Dikmedaş and D.V.M. Andaç Kılıçkap for their experimental helps throughout my *in vivo* mice experiments. They were always encouraging and friendly.

In addition to our lab members, I would like to give thanks to all members of the MBG department working in each lab; especially Nalan Yıldız, M.Sc., Hande Özünlü, B.Sc., Mehmet Can Demirler B.Sc., Ulduz Sobhiafshar M.Sc. They were always kind, helpful and supportive.

I am thankful to Ali Can Sahillioğlu M.Sc. for his crucial findings in his master thesis about ASC specks. The fundamentals of this thesis are based on his previous results.

Last but not least, I would like to express my special thanks to my family members; M.Selim Yaşa, Sevgi Yaşa, Feyza Yaşa, Reyyan Yaşa, and to my beloved secret saviour for their tremendous support from the beginning to the end of this long-running master degree. Moreover, I cannot leave unsaid the mental relief I always obtained from my old-time friends Göknil Torun and Şeyma Bilir.

ABSTRACT

IN VIVO STUDIES OF ASC SPECKS AS ANTIGEN DELIVERY VEHICLES

ASC is a 22 kDa adapter protein which is an essential component of the NLRP3, NLRC4 and AIM2 inflammasome complexes. ASC has critical functions in inflammatory and pyroptotic signaling pathways via activating caspase-1. In unstimulated cells, the ASC protein is soluble in the cytosol however upon stimulation it forms globular speck structures in close proximity to the nucleus. The importance of the ASC protein in the development of humoral immunity has been demonstrated upon vaccination of wild type and ASC knock-out mice with MF59-adjuvanted influenza vaccine. Moreover, the importance of ASC specks in cell-to-cell communication by activation of other macrophages via phagocytosis of extracellular ASC specks after pyroptosis has been demonstrated. We previously reported that ASC specks can be loaded with the model antigen ovalbumin and OVA-loaded ASC specks can be purified and fed to macrophages, which engulf the ASC-specks via phagocytosis and start degrading the protein constituents. Based on these informations, we have shown the long lasting stability of ASC specks inside the mice's bodies and its localisation to the important immune organ, spleen. Then, we checked the stimulation of immunity in *in vivo* mice studies using H5 (protein coat of *H.Influenza* virus) & OVA loaded ASC specks. Comparing the antigen specific IgG titers, we demonstrated that we can use ASC specks as H5 antigen delivery vehicle against H5N1 virus. Also, our immunisation and tumor development experiments proved that ASC specks can be used as a novel adjuvant modality in vaccine technology. Anti-tumor effect of ASC specks on tumor development provides an opportunity for us to improve ASC specks against tumor.

ÖZET

ASC ZERRELERİNİN ANTİJEN TAŞIYICI ÖZELLİĞİNİN *IN VIVO* ÇALIŞMALAR İLE GÖSTERİLMESİ

NLRP3, NLRC4 ve AIM2 enflamazom kompleklerinin esas bileşenlerinden biri olan ASC proteini 22 kDA'luk bir adaptör proteindir. ASC proteini kaspaz-1'i aktifleştirmesi ile enflamatuar ve piroptotik sinyal yolaklarında önemli işlevler üstlenmiştir. ASC proteini, uyarılmamış hücrelerde sitozolde dağınık halde bulunur iken uyarılma halinde çekirdeğe yakın mesafede toplaşarak küresel zerrecik oluştururlar. ASC proteinin hümoral bağışıklık gelişimindeki önemi doğal fenotipteki ve ASC proteini sustu-rulmuş farelerin MF59 adjuvantlı influenza aşısıyla aşılanmaları sonrasında gösterilmiştir. Ek olarak, ASC zerrelerinin hücreler arası iletişimdeki önemi piroptoz sonrası hücre dışına salınan ASC zerrelerinin fagositoz edilmesi sonrasında diğer makrofajların aktive olması ile gösterilmiştir. Daha önce ASC zerrelerinin model antijen ovalbumin ile yüklenebildiğini, OVA yüklü ASC zerrelerinin saflaştırılabildiğini ve makrofajların bu zerreleri fagositoz edebildiklerini rapor etmiştik. Ayrıca makrofajların ASC zerrelerini fagositoz yoluyla içlerine alıp yapıtaşlarına ayırdıklarını da gösterdik. Bu bilgilere dayanarak, ASC zerrelerinin fare vücudundaki uzun süren dayanıklıklarını ve önemli bağışıklık organı olan dalakta toplandığını gösterdik. Daha sonra H5 & OVA yüklü ASC zerrelerini kullandığımız fare deneylerinde bağışıklığın uyarılmasını kontrol ettik. Antijen spesifik IgG titrelerini karşılaştırarak ASC zerrelerinin H5N1 virüsüne karşı H5 gönderim aracı olarak kullanılabileceğini gösterdik. Ayrıca, bağışıklık kazandırma ve tümör oluşturma deneylerimiz ispatladı ki ASC zerreleri aşı teknolojisinde yeni bir adjuvant yöntemi olarak kullanılabilir. Tümör oluşumunda ASC zerrelerinin tümör karşıtı etkisi ASC zerrelerinin tümöre karşı geliştirilmesi için de bize bir fırsat sunuyor.

TABLE OF CONTENTS

LIST OF FIGURES

LIST OF TABLES

LIST OF SYMBOLS

a.u.	arbitrary unit
bp	Base Pairs
g	Gravity
gr	Gram
kb	Kilobase
kDa	Kilodalton
L	Liter
M	Molar
mA	Milliamper
mg	Milligram
min	Minute
ml	Milliliter
mm	Millimeter
mM	Millimolar
ng	Nanogram
oC	Centigrade degree
sec	Second
V	Volt
μg	Microgram
μl	Microliter

LIST OF ACRONYMS/ABBREVIATIONS

Ab	Antibody
AIM2	Absent in Melanoma 2
Alum	Hydrated Potassium Aluminium Sulfate
APC	Antigen Presenting Cell
APS	Ammonium Persulfate
Ar	Argon
ASC	Apoptosis-Associated Speck-Like Protein Containing a CARD
BF	Bright field
BSA	Bovine Serum Albumin
BMDC	Bone Marrow derived Dendritic Cell
CARD	Caspase Recruitment Domain
Casp1	Caspase-1
Caspase	Cysteine-Aspartic Proteases
CD	Cluster of Differentiation
CDS	Coding Sequence
cDNA	Complementary DNA
COS-7	CV-1 (simian) in Origin, and Carrying the SV40 7
CpG	C-phosphate-G
C-terminal	Carboxyl-Terminal
CytOVA	Cytoplasmic Ovalbumin
DALIS	Dendritic Cell Aggresome-Like Induced Structures
DAMP	Danger-Associated Molecular-Patterns
DAPI	4',6-diamidino-2-phenylindole
DC	Dendritic Cell
DD	Death Domain
ddH2O	Double Distilled Water
DED	Death Effector Domain
DISC	Death-Inducing Signaling Complex

DMEM	Dulbecco's Modified Eagle Medium
DMSO	Dimethyl Sulfoxide
DNA	Deoxyribonucleic Acid
dNTP	Four Deoxyribonucleotides
DRiP	Defective Ribosomal Products
dsDNA	Double Stranded DNA
EB	Elution Buffer
ECMV	Encephalomyocarditis Virus
EGFP	Enhanced Green Fluorescent Protein
Em	Emission
ER	Endoplasmic Reticulum
EtBr	Ethidium Bromide
EYFP	Enhanced Yellow Fluorescent Protein
FADD	Fas-Associated Protein with Death Domain
FBS	Fetal Bovine Serum
g.s.	Gravity Sedimentation
GST	Glutathione S-Transferase
H	Helix
hASC	Human ASC
HBS	HEPES Balanced Salt
HEK	Human Embryonic Kidney
HEPES	4-(2-hydroxyethyl)-1-piperazineethanesulfonic Acid
HRP	Horseradish Peroxidase
IL	Interleukin
IL-1β	Interleukin 1-β
LB	Luria-Bertani Broth
LPS	Lipopolysaccaride
LRR	Leucin Rich Repeat
MCS	Multiple Cloning Site
MHC	Major Histocompatibility Complex
MSU	Monosodium Urate

n.s.	Non Spesific
NACHT	NAIP, CIITA, HET-E and TP1
NEAA	Non-esential Amino Acid
neg	Negative
NF-κB	Nuclear Factor Kappa B
NLR	NOD-Like Receptor
NLRC4	NLR family, CARD Domain Containing 4
NLRP3	NLR family, Pyrin Domain Containing 3
NOD	Nucleotide-Binding Oligomerization Domain
NP	Influenze Nucleoprotein
N-terminal	Amino-Terminal
PAMP	Pathogen-Associated Molecular Pattern
PBS	Phosphate Buffered Saline
PCR	Polymerase Chain Reaction
Pen/Strep	Penicillin/Streptomycin
PFA	Paraform Aldehyde
PLA	Polylactic Acid
PLGA	Poly(lactic-co-glycolic acid)
PMA	Phorbol 12-myristate 13-acetate
proIL-18	Prointerleukin-18
proIL-1β	Prointerleukin-1β
PYD	Pyrin Domain
RCSB	Research Collaboratory for Structural Bioinformatics
RF	Reverse Flow
RIG-I	Retinoic Acid-Inducible Gene-I
RLR	RIG-I like Receptor
RPM	Rotations per Minute
RT	Room Temperature
SDS	Sodium Dedocyl Sulfate
SDS-PAGE	SDS- Polyacrylamide Gel Electrophoresis
shortASC	Short Isoform of ASC

TAE	Tris-Acetate-EDTA
TBS	Tris Buffered Saline
TBST	Tris Buffered Saline Tween
TEMED	N,N,N',N'-Tetramethylethane-1,2 diamine
TLR	Toll-Like Receptor
Tris	Tris(hydroxymethyl)aminomethane
Tween	Polysorbate
UBB	Ubiquitin B
UV	Ultraviolet
v	Volume
w	Weight
WT	Wild-Type

1. INTRODUCTION

1.1. The immune system

Biological systems use immune responses to fight against potentially deadly infections caused by variety of pathogens such as bacteria, viruses, parasites and fungi. Adaptive immunity is the specific immune response developing from birth as an adaptation to infection. Immunological memory can be result from adaptive immunity which provides life long protective immunity from reinfection with the same pathogen. For proper activation of adaptive immunity, innate immune response is essential [1].

1.1.1. Innate immunity

PAMPs (pathogen associated molecular patterns) are evolutionary conserved structures on pathogens such as bacterial lipopolysaccharides (LPSs) and endotoxins found on the cell membranes of bacteria. On the other hand, DAMPs (danger associated molecular patterns) are composed of nuclear or cytosolic proteins such as heat-shock proteins, HMGB1 (high-mobility group box 1), ATP, uric acid, heparin sulfate and DNA. Those different types of DAMPs and PAMPs are detected at low concentrations by pattern recognition receptors (PRRs) in a quick fashion by innate immune system [2]. In this type of immunity pathogen-specific receptors are found already encoded in the germ line. Innate immunity is orchestrated by a diverse set of membrane bound and cytoplasmic pattern recognition receptors [3]. Toll-like receptors (TLR) are membrane bound receptors found in plasma and endosomal membranes. Every TLR specificly recognizes a particular pathogenic motif. For example, TLR4 is most well-known for recognizing lipopolysaccharide (LPS), a component present in many Gram-negative bacteria. Notably, it is shown that those TLR agonists can be used as an adjuvant to activate antigen presenting cells (APCs) in vaccine development [4]. Other PRRs are RIG-like receptors (RLR), NOD-like receptors (NLRs) and absent in melanoma 2 (AIM2) receptor which are cytoplasmic.

1.1.1.1. Inflammasome activation. It is accepted that after the pathogen recognition by a small number of NLRs (NOD-like receptor family), inflammasome activation occurs by oligomerization of inflammasome components. If the inflammasome complex does not assemble correctly it may lead to autoimmune disorders and cancer. The initiation of the assembly starts with self assembly of several NLR family such as NLRP3, NLRC4, NLRP1/ 6/ 7/ 12. Conformation change in NLRs abrogates the LRR inhibition on NATCH domain which is followed by oligomerization of NLRs via their NATCH domains. NLRC3 can activate procaspase-1 with the help of its CARD (caspase recruitment domain). Since NLRP3 (the mostly studied NLR) does not contain the CARD, it needs ASC (apoptosis-associated speck-like protein containing a CARD) as an adaptor protein which interacts with zymogen procaspase-1 to let them cleave themselves (induced proximity model) [2]. Then, the proIL-1beta and proIL-18 can be hydrolized by mature caspase-1 to be secreted from the cell [5, 6].

1.1.1.2. Recognition of viruses by inflammasomes. Two signals are required for inflammasome mediated cytokine release. The first signal upregulates the expression of proIL-1β, proIL-18, NLRP3 at the mRNA and the protein levels. This signal is transmitted by TLR, IL-1R, TNF receptor via activation of NF-κB signalling. This pathway activation increases cellular levels of NLRP3 as well as immature forms of cytokines proIL-1β and proIL-18. Upregulation of proIL-1β and proIL-18 synthesis is not sufficient for their processing and release. Thus, a second signal is needed to accomplish the process. The second signal induces the activation of caspase-1. Up to now, PYHIN (pyrin and HIN domain-containing protein) family member AIM2 inflammasome classes, RIG-I and NLRP3 are known to play role in viral recognition. It is shown that RNA activates the RIG-I inflammasome. The AIM2-like receptors bind to viral DNA and adaptor protein ASC to activate PYHIN inflammasome. The AIM2 inflammasome is shown to be activated by intracellular double-stranded DNA (dsDNA) derived from DNA viruses. Distinctively, NLRP3 inflammasome is activated by a wide range of stimuli, including endogenous metabolites, bacterial components, and environmental irritants, in addition to viruses. Those specific activation of different inflammasomes following the innate recognition of viruses via PRRs plays a key

role to restrict viral replication at the initial phase of infection and also to initiate antigen-specific adaptive immune responses [7].

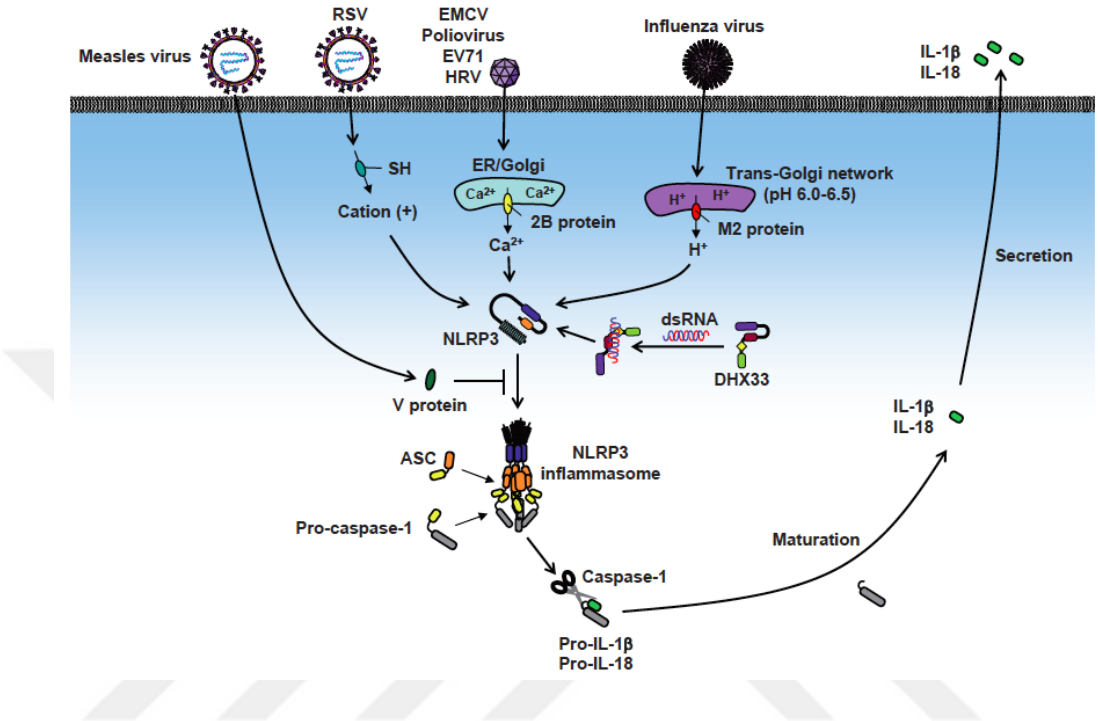

Figure 1.1. Recognition of RNA viruses by nucleotide-binding domain and leucine-rich-repeat-containing protein 3 (NLRP3) inflammasome (Adopted from Yamazaki, 2014) [7].

1.1.2. Adaptive immunity

The acquired/ specific/ adaptive immune system is highly specialized and systemic so that it can eliminate and prevent pathogen growth. The adaptive immunity is the second level strategy after the innate immunity. Distinctively, immunological memory is formed after the first exposure to a specific pathogen, which provides an enhanced response to fight against an infection by destroying the invading pathogens and any toxic molecules they produce. The basis of vaccination relies on this immune strategy via using antigens to elicit the adaptive immune response.

T lymphocytes use T cell receptors (TCR) and B lymphocytes use immunoglobulins (Ig) to detect non-self agents during the adaptive immune response. Ig can

bind to free molecules, but TCR can only bind to degraded antigenic particles which are loaded and presented on the major histocompatibility complex (MHC) proteins. Allelic polymorphisms provide for the great variation of MHC molecules. The recombinase activating gene (RAG) products and terminal deoxynucleotidyl transferase (TdT) perform gene rearrangement and junctional diversity to ensure Ig and TCR diversity. Thus, TCR, Ig, MHC molecules, RAG products and TdT are the molecules designating the adaptive immunity [8].

1.2. Antigen presentation pathways

The adaptive immunity and the innate immunity systems work together to fight against an infection. T lymphocytes are needed to be activated by innate immune cells through antigen presentation. Major histocompetibility complexes (MHC) of APCs provide the presentation of degraded antigen particles to T cells. This process is improved by nearly all innate immunity pathways triggered by pattern recognition receptors (PRRs). Adjuvants are used in vaccines to provide sufficient antibody production. Alum is the adjuvant used mostly in vaccines and has been shown to exert its adjuvant activity via stimulation of NLRP3 inflammasome in an ASC dependent manner [9].

1.2.1. MHC class I and MHC class II mediated antigen presentation pathways

Vaccine antigens are engulfed by immature dendritic cells (DCs) and tissue macrophages. This process leads to their activation and local inflammation which then provides their migration to the draining lymph nodes. During this migration, DCs change their surface molecule expression and mature. Engulfed antigens are processed in phagolysosome and degraded into particles in order to be loaded onto MHC (HLA in humans) molecules which display on the cell surface. It is known that phagocytosed antigens are loaded onto MHC class-II molecules, and antigens produced from infected cell is loaded onto MHC class-I molecules. Moreover, while CD4+ T cells recognize antigens presented from class II MHC molecules, CD8+ T cells recognizes antigens presented from class I MHC molecules. Any region of an antigen can generate T cell

epitope. Yet, B cell epitopes can be only generated by surface parts of the antigen. MHC epitope signal itself is not enough for T cell activation, also there is a need of a costimulation by an activated DC [10].

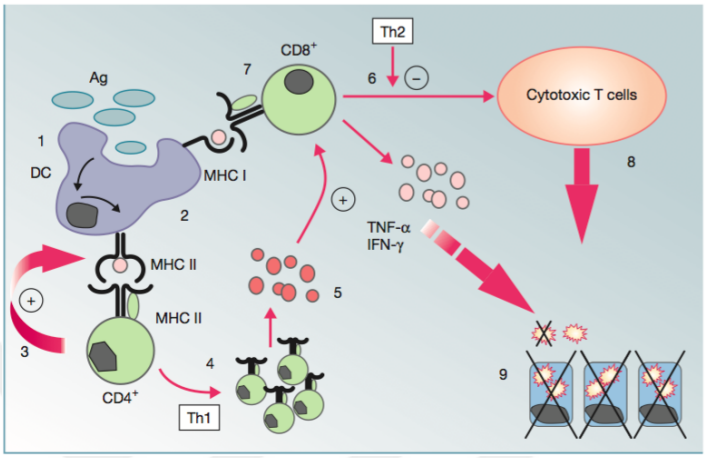

Figure 1.2. Generation of T cell effector responses (Adopted from Siegrist, 2008) [10].

1.2.2. Antigen presentation process and inflammasomes upon influenza virus infection

The way of influenza viral infection eradication is through inflammasome dependent adaptive immunity. After respiratory DCs are infected with influenza virus, caspase-1 is activated which leads to IL-1beta secretion and causes cell death through pyroptosis. Inflammatory signals activate bystander DCs. In order to activate CD8+ T cells, they start to engulf antigens and migrate from the lung to the mediastinal lymph nodes (mLNs). Pro-IL-1beta, pro-IL-18, and NLRP3 expression is introduced by signals from gut-resident microbiota [7].

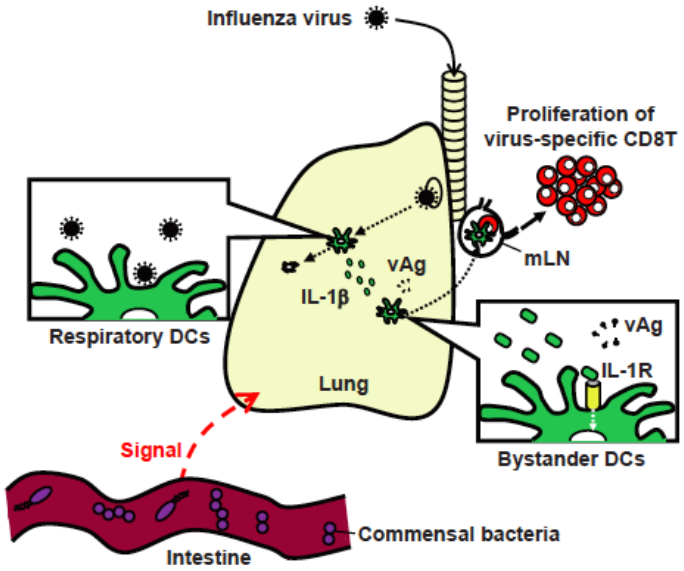

Figure 1.3. Proposed model of inflammasome-dependent induction of adaptive immunity against influenza virus infection (Adopted from Yamazaki, 2014) [7].

1.3. ASC protein

Only several cytoplasmic PRRs (ex., NLRP3, NLRC4, AIM2) detect PAMPs and become part of inflammasome complexes. It is known that the NLRP3 inflammasome can be activated by pore-forming toxins, particulate materials, and extracellular ATP which proceeds with potassium efflux, lysosomal damage, and reactive oxygen species (ROS) production [11]. ASC protein acts as an adaptor protein in NLRP3 and AIM2 inflammasome formation by making receptor and procaspase-1 interaction possible. This inflammasome activation is followed by rapid formation of micrometer sized compact aggregosome like perinuclear structure, which is called ASC speck [12]. Role of ASC speck in proximity mediated procaspase-1 self activation is shown.

1.3.1. Structure of ASC protein

ASC is a 22kDa, 196 amino acids long protein having an N-terminal pyrin domain (PYD) and a C-terminal caspase recruitment domain (CARD) linked with 23 amino

acids long flexible linker [13, 14].

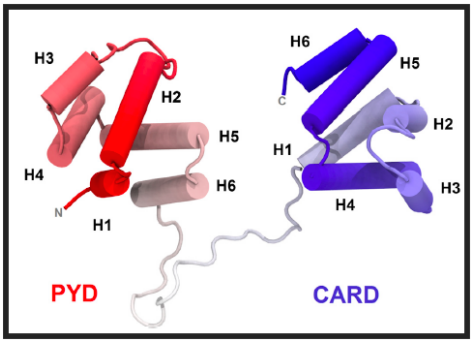

Figure 1.4. NMR structure of ASC protein (Adopted from de Alba, 2009) [14].

These two domains of the ASC protein belong to the death fold super family, which have a 6-helix bundle conserved motif structures. These motifs are found in proteins playing critical roles in apoptosis and inflammatory pathways. There are long (main transcript responsible for the compact shape) and short isoforms (responsible for filament formation) of ASC mRNA in humans. IL-1 beta secretion after procaspase-1 activation can be recruited by the short isoform of ASC protein. We have elucidated that certain mutations in Type-I surfaces disrupt the speck structure. This founding shows that PYD-PYD and CARD-CARD proper interactions are the main reason for the ASC speck formation which may also explain its rapid assembly with respect to other aggresome formations [15].

1.3.2. ASC speck formation

There are different kinds of inflammasomes, and each of them are activated by different stimuli. The cryopyrin (NLRP3) inflammasome can be activated by wide range of signals like intracellular bacteria infection, ATP, nigericin or maitotoxin, danger signal monosodium urate (MSU), antiviral compounds R837 and R847, bacterial RNA and viral double-stranded RNA [16]. It is shown that ASC assembly is downstream of inflammasome activation. ASC has direct effects on caspase-1 activation and pyroptosis. Thus, this supramolecular complex is called pyroptosome. Cryopyrin is not found in the ASC pyroptosome structure, yet ASC dimers and caspase-1 presence

is shown. From this information it is suggested that inflammasome formation may be an initial catalyst to start ASC dimerization, then those ASC dimers dissociate to oligomerize more to form a bigger structure; the pyroptosome. As a response to proinflammatory stimuli, each macrophage formed one pyroptosome within 3 minutes which are 1-2 micrometer sized speck, crystal-like structures next to the nucleus [17].

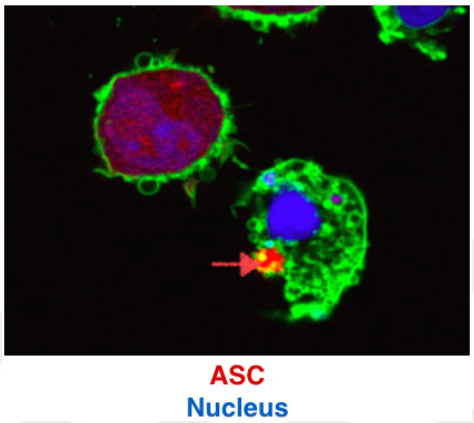

Figure 1.5. ASC speck formation upon infection (Adopted from Franklin, 2014) [18].

Moreover, the ASC pyroptosomes are shown to be formed spontaneously in cell-free lysates at 37°C incubation. Also, caspase-1 activation is observed within those pyroptosome activated cell lysates in a hypotonic solution [17].

1.3.3. Extracellular activity of ASC speck

We have previously shown that ASC specks are released with IL-1 beta secretion after inflammasome activation and accumulated in the extracellular space [15]. These secreted ASC specks are ingested by macrophages and activate caspase-1 after engulfed by wild-type, ASC-deficient (Pycard$-/-$) or NLRP3-deficient (Nlrp3$-/-$) macrophages [19]. ASC injection causes acute inflammatory reactions in mice. It is suggested that autoantibodies against ASC increment increased the engulfment capacity and IL-1 beta secretion of macrophages [18, 20]. The quick formation of the ASC specks followed by cell death calls for other resident cells toward newly generated specks. Moreover, Sahillioğlu A. in our laboratory showed the perfect stability of ASC specks *in vitro* and *in vivo*. They are long-lasting, slowly degraded structures.

1.3.4. Artificial loading of ASC specks with antigens

It is shown that ASC protein has inflammasome dependent and independent roles in antigen presentations [9]. The importance of the ASC protein in the development of humoral immunity has been demonstrated upon vaccination of wild type and ASC knock-out mice with MF59-adjuvanted influenza vaccine. [21]. As in dendritic cell aggresome like induced structures (DALIS) which are shown to make protein aggregation that makes them an important tool in antigen presentation [22], ASC specks are shown to co-aggregate with cytosolic proteins. This aggregation appeared to be because of nonspecific hydrophobic interactions [15]. Especially the ubiquitinated proteins having hydrophobic patches shown to co-aggregate on ASC speck. Likewise, ASC speck is thought to have a potential implications in antigen presentation [15]. We have patented the finding that the ASC specks can be used as an antigen delivery vehicle on 24.04.2012 with the reference number 32178-01 and a corresponding international application (PCT IB2013/053079).

1.4. Immunization/ Vaccination

Over the course of millennia people have died in hundreds of thousands & millions due to infections by pathogens &viruses. One of the world's most infectious disease leading to death of 1/3 infected people was smallpox. Only within 20th century, about 300 million people died. Vaccine against this virus globally eradicated the disease since 1979. Bubonic plague is another deadly infectious disease caused by *Yersinia pestis* bacteria. 30 to 90% people would die within 10 days from this infection without treatment. Vaccine against bubonic plague has not been found yet. Another deadliest disaster in human history is caused by spanish flue pandemics. This viral infection killed 3 to 5% of the world's population. Thanks to the scientific researches, immunization is developed to combat their spread. Vaccination, also called immunization, is a targeted induction of an immune response which provides production of antibodies against a particular pathogen. Scientists take advantage from the immune system's nature to manipulate the immune system effectively. The trick of immunization is introduction of a part of a pathogen (antigen) or attenuated pathogen in order to develop

protective immunity against that immunogen without infecting the individual [1].

1.4.1. Importance of vaccines

At the present time, a vast majority of human deaths are caused by infectious diseases particularly in low-income countries. This situation shows the relation between health and the economy. This disparity can only be solved by vaccination thus reducing the health-care costs via controlling and eliminating the deadly diseases. Through immunization morbidity and mortality rate in childhood decreased, which improved social and economic life of the families. Also, vaccination lead to increased avarage life-span [23].

If the global vaccination coverage would be improved, an additional 1.5 million death would be averted every year. Approximately 2 to 3 million deaths from diphtheria, tetanus, pertussis (whooping cough), and measles are prevented by vaccination. Although the implementation of intensive vaccination policies and preventive public health measures has caused a significant decline in the prevalence of many important infectious diseases, several community-acquired infections, including brucellosis, tularaemia, and CCHF, remain important health challenges in Turkey. According to the data released by the Statistical Institute of Turkey, 4226 patients lost their lives because of infectious diseases in Turkey in 2008. In Turkey population, brucellosis has a prevalence rate of 25 per 100 000, tularaemia has become an emerging zoonotic disease, tuberculosis has a prevalence rate of 24 per 100 000 having a steady decline within 15 years, hepatitis A virus (HAV) -still a childhood disease- and acute hepatitis B virus (HBV) infection prevalence rates were 5.21 and 3.79 per 100 000. HAV prevalence is expected to decline with the help of recently included HAV vaccine in the National Immunization Programme of Turkey. Although prevalence was high in Turkey, no case was detected since 2010 [24].

Chart. National Immunization Chart (National Immunization Schedule) Vaccines of the Ministry of Health of Turkey (0-18 age) - 2015*

	Birth	1. month	2. month	4. month	6. month	12. month	18. month	24. month	Elementary 1. grade or age 4-6	Elementary 8. grade or age 10-12
Hepatitis B (BHA)	I	II			III					
BCG			I							
aBDT-IPA-Hib			I	II	III		IV (R)		aBDT-IPA (R)	dT (R)
OPA					I		II (R)			
Pneumococ (KPA)			I	II	III	IV (12-18 months) (R)				
KKK						I			II (R)	
Varicella (SA)						I				
Hepatitis A (AHA)							I	II		

Additional Chart. Additional Vaccines on the National Immunization Schedule Vaccines of the Ministry of Health of Turkey (0-18 year of age)-2015*

	Birth	1. month	2. month	4. month	6. month	9. month	18. month	24. month	Elementary 1. grade or age 4-6	Elementary 8. grade or age 10-12
Rotavirus (RVA)			I	II	(III)					
dapT, dapT-IPV										Preferably instead of DT, one dose
Human Papilloma Virus (HPA)										Used instead of dT, one time Between 9-18 years 3 doses in total
Influenza (IIA)						Every year after the 6th month (age-appropriate dose and number)				
Meningococcal (KMA4)							Within the framework of practical recommendations, 1 or 2 doses after informing the families			

Figure 1.6. National Immunization Chart (National Immunization Schedule) Vaccines of the Ministry of Health of Turkey (0-18 age) - 2015 (Adopted from Arısoy, 2015).

1.4.1.1. Influenza A virus subtype H5N1. One of the contagious virus as having a high lethality rate is the Influenza virus. It is known that avian influenza (H5N1) kills over half the humans it infects. At least partially effective way to avoid influenza viral infection is vaccination with the seasonal flue vaccine. The H5N1 subtype is an RNA virus. The name of H5N1 comes from the HA(hemagglutinin) and NA(neuraminidaze) types of influenza A virus to differentiate this subtype from the others. Variations in HA and NA parts provide species-selectivity of various influenza strains [25].

As an immunization strategy, the virus coat protein HA is used in vaccines in order to mimic the viral infection to educate the immune system by production of virus specific antibodies. HA is a good candidate to mimic the virus itself, since HA is an antigenic glycoprotein found on the surface of the influenza viruses which is responsible for binding the virus to the cell that is being infected. Meta-analyses demonstrated

that inactivated vaccines have 60% efficacy in children and 40% efficacy in adults and the elderly, while a more recent meta-analysis demonstrated that efficacy was lower then the previous report [26, 27].

Current vaccines can provide only partial protection against the influenza viruses. Yet, these vaccines must be formulated every year. Because, RNA viruses have high mutation rates, which is caused by genetic recombination when a host is infected with two different influenza strains at the same time. This may lead to influenza pandemics after passing this strain between humans [28].

Certain number of combined considerations are needed for a newly found vaccine to be recommended widely. H5N1 vaccines are developing technologies and their safety, immunogenicity, degree and duration of their protective effects are comparatively restricted. Although there have been no major safety concerns identified for H5N1 vaccine usage up to now, significant safety datas are needed. At comparable antigen dosages, the immunogenicity of the vaccines must be similar. Antigen concentration can be lowered with adjuvant usage, yet some vaccines (inactivated) do not need an adjuvant to be effective. The relationship between the measurable markers of immune responses to H5N1 vaccines and protection is not clear. Currently, there are no data from human trials on how well H5N1 vaccines may protect against disease. Only a few studies have considered the potential of H5N1 vaccine on its duration of protection [29].

1.4.1.2. Hemagglutinin. Influenza viruses contain hemagglutinin (HA) glycoproteins as a coat protein on the surface. These HA glycoproteins provides virus binding to sialic acid found on cell membranes. Since erythrocytes and cells in the upper respiratory tract have sialic acid, influenza viruses mostly effect those parts in the body via viral envelope fusion with the endosomal membrane which is provided by HA [30]. There are at least 18 different HA antigens named H1 to H18. H1,H2,H3 are present in human influenza viruses. Although H5N1 virus does not infect humans, single aminoacid change in this strain provides their receptor binding to human cells, thus the infection

[31].

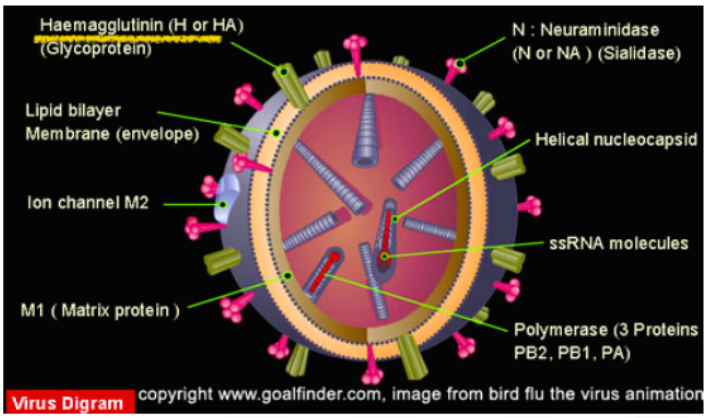

Figure 1.7. Structure of influenza, showing neuraminidase marked as NA and hemagglutinin as HA.

1.4.2. Types of vaccines

There are four types of vaccines depending on the nature of their antigens; live attenuated, killed inactivated, toxoid, and subunit variety.

1.4.2.1. Live attenuated vaccines. In order to attenuate a viral pathogen, the virus can be grown in an artificial growth medium at a lower temperature than the human body or in a foreign host. This approach was developed to be advantageous from the feature of RNA viruses which have high mutation rates. This will provide the formation of mutant viruses which will show reduced virulence factors for human and decreased proliferation rate in human body. To do so, the human immune system will be immunized with this kind of attenuated pathogen and then it will be eliminated before the spread of the virus [32].

1.4.2.2. Killed/inactivated vaccines. While the killed type is used for bacterial vaccines (typhoid), inactivated is used for viral vaccines (polio, hepatitis A). As their name suggests, the bacteria or the virus are no longer alive when immunization is ap-

plied. Since the pathogens can no longer multiply, vaccination should be done several times to boost adaptive immunity. The most important disadvantage of this type of vaccination is their inability to give rise to cytotoxic T cells [32].

1.4.2.3. Toxoid vaccines. Some of the disease causing pathogens (Tetanus) do their job by exotoxin secretion. Bacterial growth leads to the secretion of their toxins. When they are lysed, the toxins will be obtained. Treatment of the toxins with formaldehyde leads to changes in their aminoacid and the conformational changes in the protein structure. After filtration processes, the pure non-toxigenic antigen can provide immunity as the natural toxin does [32].

1.4.2.4. Subunit vaccines. In this approach, only a part of a pathogen (the most antigenic part) is used, which is sufficient for antibody production in the host to prevent a possible infection. Protein antigens and polysaccaride antigens can be used for subunit vaccine development that can be T-dependent or not, respectively. Subunit vaccines are more bio-safe than the other type of vaccines as they do not include the whole pathogen during injection which can cause overactivity, thus septic shock [32].

1.5. Antigen delivery systems

Inactivated or live attenuated vaccines containing the whole pathogen are good enough to induce immune responses without the need of any adjuvants. Adjuvants may lead to overreaction in humans, thus are not bio-safe. Because of this reason, scientists develop new approaches to produce vaccines which consists of the most antigenic part of a pathogen having the homologous epitopes capable of inducing protective immunity, which is called subunit vaccines. Yet, subunit vaccines are poor in inducing immune response and needs repeated vaccinations. Antigen delivery systems provide controlled release of antigens [33].

There are different kinds of antigen delivery systems, which can be biodegradable or not. Their common ground is to ease engulfment of antigens by Antigen Presenting

Cells (APCs) via increasing the size of the antigens. There are two types of energy-dependent endocytosis; phagocytosis and pinocytosis. Phagocytosis is the mechanism where APCs engulf the pathogen and fuse them with the phagolysosome, thus degrade them into particles. Only after this process, the degraded particles can be loaded onto MHC molecules to induce further immune responses. In order for phagocytosis to occur the engulfed particle's size must be between 0,5 - 10 micrometer [34]. Particle size less than 0,5 micrometer leads to pinocytosis, which cannot induce immunity. Thus, in subunit vaccine development the antigen delivery systems are important to increase the antigen size and extend antigen degradation time to increase the capacity of antigen presentation to T cells. Mostly liposomes and hydrogels are used for antigen delivery, although their degradation time and shelf lives are really short.

1.5.1. Ingredients of vaccines

Many severe and fatal bacterial infections were observed in vaccinated children in the early 20th century. After those serious incidences preservatives were included as a vaccine ingredient in order to prevent possible bacterial or fungal contaminations [35]. Although subunit vaccines are the safest kind of vaccine strategy, they are poor in immunogenicity. In order to enhance the immune response, adjuvants started to be used in vaccines. Aluminium salts are the initial adjuvant found to be reducing the rate of antigen release at the site of inoculation which is called "depot effect". This depot effect has high a importance for any vaccine to be effective. Adjuvants provide improved antigen uptake by APCs, thus activates APCs, and promotes their cytokine production [35]. Additives are included as vaccine ingredients in order to protect them from adverse conditions like freezing, drying, and heat. Moreover, additives are needed to avoid the antigens' adherence to the sides of the vials [35]. In the final product of a vaccine, inactivating agents (formaldehyde), antibiotics, and cellular residuals (egg and yeast proteins) can be found [35].

1.5.2. Drawbacks of current vaccines

Every kind of vaccine has its own storage conditions. Most of them can be stored at -80 to +2°C for one year. Transfer of the current vaccines to another facility is difficult because of the need of proper vaccine carriers which can provide -80 to +2°C protection. In addition to difficulty in storage conditions, shelf lives of vaccines are really short. Depending on the type of the vaccine's shelf life can vary from 1 to 2 years, also some of them must be kept in the dark. Some of the vaccines, which are freeze dried, need reconstitution with appropriate solutions. Most importantly, the safety of Alum (the only accepted adjuvant) usage in vaccines is a controversial topic [36].

2. PURPOSE

Based on studies of our laboratory around the inflammasome complexes and their activation principles over the last ten years, we have developed molecular biological know-how and we discovered a novel antigen delivery/adjuvant modality. In this project we aim to demonstrate the competency of our purposed model "ASC specks" in *in vivo* studies.

The first purpose of this project is to load the ASC specks with antigens (ovalbumin and H5 coat protein of *H.influenza*) and achieve vaccination. To this end, we have developed H5-ASC and OVA-ASC fusion constructs in pcDNA3 vector backbone and after transfection into HEK293T cell line we purified the antigen loaded specks. In order to achieve vaccination, we did medium scale production of H5 and OVA loaded ASC specks in HEK293T cell culture. Competency of loaded specks are checked after C57/BL6 mice immunization studies via antigen specific IgG titer comparisons.

The second purpose of this project is to elucidate the possible role of ASC specks as a novel adjuvant modality. For this aim, we have designed H5 and OVA immunization experiments with a known adjuvant "Freund's" to compare the adjuvant effect of ASC specks in C57/BL6 mice.

The last purpose of the project is to check the effect of ASC specks on tumor development in order to observe whether ASC specks have a potential anti-tumor activity. Therefore, we made EG.7-OVA tumor development on the flank of C57/BL6 mice and did OVA-ASC intraperitoneal injections to observe tumor decrement.

3. MATERIALS

3.1. Cell Lines

Table 3.1. Cell lines used in this study.

	Catalog number	**Main Source**	**Provider**
HEK293(F)T	R700-07	Invitrogen, USA	Kindly provided by Prof. Maria Soengas
THP-1	ATCC TIB-202	ATCC, USA	Kindly provided by Prof. Ahmet Gül
EG.7/EL4(OVA)	ATCC CRL-2113	ATCC, USA	Kindly provided by Prof. İhsan Gürsel

3.2. Chemicals, Plastic and Glassware

Chemicals were purchased from either Sigma-Aldrich (USA), Merck (Germany) or AppliChem (Germany), plasticware from TPP (Switzerland) for cell culture, tips and tubes from Axygen (USA). All glassware, tips and tubes were autoclaved at 121°C for 20 minutes for sterilization prior to use.

3.3. Buffers and Solutions

3.3.1. Cell Culture

Table 3.2. Solutions and media used in cell culture.

0.5 Trypsin-EDTA 10X	Gibco Invitrogen, USA
DMSO	AppliChem, Germany
Dulbecco's Modified Eagle Medium (DMEM)	Gibco Invitrogen, USA
Fetal Bovine Serum (FBS)	Gibco Invitrogen, USA
MEM Non-essential amino acid (NEAA) 100X	Gibco Invitrogen, USA
Penicillin/Streptomycin 100X (5000 u Penicillin + 5000 μg Streptomycin per ml)	Gibco Invitrogen, USA

Table 3.3. Buffers used in cell culture.

Freezing Medium	20 FBS, 1X Pen/Strep, 100μM MEM-NEAA, 7.5 DMSO
PBS 10X	80 gr NaCl, 2 gr KCl, 2.4 gr KH2PO4, 14.4 gr Na2HPO4, Add ddH2O upto 1 lt (pH 7.2)

3.3.2. Cloning and Analytic Digestion

Table 3.4. Enzymes used for cloning.

Restriction Enzymes (HindIII)	NEB, USA
T4 DNA Ligase	NEB, USA
Q5® High-Fidelity DNA Polymerase	NEB, USA
Alkaline Phosphatase, Calf Intestinal (CIP)	NEB, USA

3.3.3. Agarose Gel Electrophoresis

Table 3.5. Buffers and solutions used for agarose gel electrophoresis.

50X Tris Acetic acid EDTA (TAE)	2 M Tris-acetate, 50 mM EDTA pH 8.5
DNA Ladder	DNA Ladder Mix Fermentas, USA
Ethidium Bromide (EtBr)	Merck, USA
Loading Dye	6x Loading Dye Fermentas, USA

Table 3.6. Solutions for liquid and solid bacterial culture.

LB Agar (Solid culture, autoclaved)	1 L LB medium, 15 g Agar
LB Medium (1 L) (Liquid culture, autoclaved)	10 g Tryptone, 5 g Yeast Extract, 5 g NaCl
Ampicillin (1000X = 100 mg/ml in 70 EtOH)	AppliChem, Germany
Kanamycin (1000X = 50 mg/ml in ddH20)	Sigma-Aldrich, USA

3.3.4. Transfection of human HEK293T cells via calcium phosphate method.

Table 3.7. Buffers and solutions used in transfection.

2X HBS Buffer	50 mM HEPES pH 7.0, 280 mM NaCl, 1.5 mM Na2HPO4
Chloroquine	AppliChem, Germany
HEPES	Gibco Invitrogen, USA

3.3.5. Western blotting

Table 3.8. Chemicals for western blotting.

Lumi-Light Western Blotting Substrate	Roche, Switzerland
SDS	AppliChem, Germany
TWEEN	CalbioChem, Canada
Protein Ladders	PageRuler Prestained (SM0671) Fermentas USA, PageRuler Prestained (26616) Thermo USA

Table 3.9. Recipes for western blotting.

Acrylamide:Bisacrylamide	29.2 gr Acrylamide, 0.8 gr bisacryalmide in 100 ml
Ammonium Persulfate	10% APS (w/v)
Blocking Solution	5% BSA in TBS-T
Coomassie Blue Staining Solution	0.1% Coomassie Blue, 10%Acetic acid, 50% Methanol in ddH2O
Coomassie Blue Destaining Solution	10% Acetic acid, 40% Methanol in ddH2O
Lysis buffer for sonication	1X PBS including 2mM, EDTA+ protease inhibitor cocktail
15% Resolving Gel Stock	50 ml 30% Acrylamide, 1 ml 10% SDS, 20 ml 1.875M Tris 8.8, 29 ml ddH2O
15% Resolving mini gel	4 ml 15% Resolving gel, 40 μl 10% APS, 4 μl TEMED
Running Buffer	1X Tris-Glycine buffer, 0.1% SDS
6X Laemmli Sample Buffer	1.2 gr SDS, 0.9 gr DTT, 6 mg BPB, 4.7 ml Glycerol, 1.2 ml Tris 0.5M (pH 6.8), 2.1 ml ddH2O
4% Stacking Gel Stock	3.3 ml 30% Acrylamide, 250 μl 10% SDS, 6.3 ml 0.5 M Tris (pH 6.8), 15 ml ddH2O
4% Stacking gel	1 ml 4% Stacking gel, 10 μl 10% APS, 1 μl TEMED
10X TBS	90 gr NaCl, 121.14 gr Tris base, Add ddH2O upto 1 L (pH 7.5)
TBS-TWEEN	1X TBS, 0.1% TWEEN 20
10X Tris-Glycine Buffer	15 gr Tris-Base, 72 gr Glycine, in 0.5 L ddH2O

3.4. Fine Chemicals

3.4.1. Antibodies

Table 3.10. Antibodies used in this study.

anti-FLAG	2368S, CST, USA
anti-ASC (monoclonal)	Kindly provided by Prof. Masumoto, Japan
anti-ASC (polyclonal)	AKIL, Turkey
anti-caspase-1	sc-515, Santa Cruz
anti-eGFP	Vatoz, Turkey
anti-mCherry	Kindly provided by Assoc. Prof. Çelik, Turkey
anti-mouse IgG, HRP	7076S, CST, USA
anti-OVA	
anti-TCRbeta H57 FITC	Kindly provided by Prof. Erman, Turkey
anti-B220 PE	Kindly provided by Prof. Erman, Turkey
anti-CD8a FITC	Kindly provided by Prof. Erman, Turkey
anti-CD8a Alexa647	Kindly provided by Prof. Erman, Turkey
anti-CD4PE	Kindly provided by Prof. Erman, Turkey
Leu4 Fitc	Kindly provided by Prof. Erman, Turkey
Leu4 PE	Kindly provided by Prof. Erman, Turkey
2.4G2 FT	Kindly provided by Prof. Erman, Turkey

3.4.2. Plasmids

Table 3.12. Other plasmids used in the project.

pmCherry-C3-hASC	AKİL, Boğaziçi University, TURKEY
pcDNA3-hASC	Nunez Lab, University of Michigan, USA
pOVA(1-235)-C3-hASC	AKİL, Boğaziçi University, TURKEY

Table 3.11. Plasmids cloned for this project.

pEGFP-C3-H5
pcDNA3-H5(69-133)-ASC
pet30a+H5

Table 3.13. Primers used in the study.

CMV-F	CGCAAATGGGCGGTAGGCGTG
Hind3-H5-F	GCG CAA GCT TAT GGA GAA AAT AGT GCT TCT T
Hind3-H5-R	ATT AAA GCT TTC ATC AAT TTC TGC ATT GTA ACG ACC
H5 69-133 F	AAG GGC TAG CAT GGA GAG ATT GTA GTG TAG
H5 69-133 R	CCC CCA AGC TTG GGA TGA TCT GAA TTT TC
M13F Universal	GTAAAACGACGGCCAGT
M13R Universal	GCGGATAACAATTTCACACAGG
M13F-pUC Universal	GTTTTCCCAGTCACGAC
M13R-pUC Universal	CAGGAAACAGCTATGAC
GFP F	CAAGCAGAAGAACGGC
H5 R	CAAAATTAGAGGCTTC

3.5. Kits

Table 3.14. Kits used in the study.

High Pure PCR Purification Kit	Roche, Switzerland
High Pure Plasmid Isolation Kit	Roche, Switzerland
Genopure Plasmid Midi Kit	Roche, Switzerland
Genopure Plasmid Maxi Kit	Roche, Switzerland
His-Trap Column Purification Kit	GE Healthcare, Sweden

3.6. Equipment

Table 3.15. Equipments used in this study.

Agarose Gel Electrophoresis	Thermo Scientific, USA
Agarose Imaging	Gel Doc XR System, Bio Rad, USA
Autoclaves	MAC 601, Eyela, Japan-ASB260T, Astell, UK
Centrifuges	Allegra X22-R, Beckman, USA-Himac CT4200C, Hitachi Koki, Japan-J2-MC Centrifuge, Beckman, USA-J2-21 Centrifuge, Beckman, USA
Freezers	2021D, Arçelik, Turkey-4250T, Arçelik, Turkey
Incubator	Hepa ClassII Forma Series, Thermo, USA
Heat Block	VWR, USA
Laminar Flow Cabinets	Class II A, Tezsan, Turkey-Class II B, Tezsan, Turkey
Magnetic Stirrer	Yellowline MSH Basic, USA

Table 3.16. Equipments used in this study.

Microscopes	Zeiss, Axio Observer, Germany-Z1 Inverted Mic., USA-Leica, TCSSP5II, Germany-Nikon, Eclipse TS100, Japan
Microwave oven	Arçelik, Turkey
pH meter	H221, Hanna Instr., USA
Pipettes	Gilson, USA
Plate reader	VersaMax, Molecular Devices, USA
Sonicator	Sonoplus, Bandelin, Germany
Spectrofluorometer	Cary Eclipse, Agilent Technologies, USA
Pipettors	Greiner-bio one, UK-RatioLab acupetta, Germany
Power Supplies	EC135-90, Thermo Electron Corp-Power Pac Universal, BIO-RAD, USA
Western blot visualization	Stella, Raytest, Germany
Scales	Precisa XT4200C, Germany
SDS-PAGE Electrophoresis System	Mini-PROTEAN 4Cell, BIO-RAD, USA
SDS-PAGE Transfer System	Mini Trans-Blot® Electrophoretic Transfer Cell BIO-RAD, USA
Shakers	Polymax 1010 , USA-Polymax 1040 , USA-Heildophl, Germany
Spectrophotometer	Nanodrop ND-100 , Thermo, USA
Vortex	Fisons Whirli Mixer, UK-GmcLab, Gilson, USA
Water Bath	GFL, Germany-Memmert, Germany
Water filter	UTES, Turkey

4. METHODS

4.1. Molecular Cloning

4.1.1. Plasmid DNA isolation

Plasmid DNA isolation was conducted according to manufacturer's instructions (Table 3.15). 6 ml of bacterial liquid culture for mini-scale, 300 ml liquid culture for midi-scale and 500 ml liquid culture for maxi-scale DNA isolation were used. In mini-scale DNA isolation, DNA was eluted from the mini-spin column using 30 μl EB. For midi and maxi-scale DNA isolations, DNA was resuspended in 200 μl ddH20.

4.1.2. High-fidelity PCR reaction

DNA fragments to be cloned into plasmid vectors were amplified using the Q5® High-Fidelity DNA Polymerase, NEB, USA). PCR reactions were carried out according to manufacturer's instructions. The protocol is summarized in Table 4.1.

Table 4.1. PCR protocol using the Q5 polymerase.

Step no	Description	Temperature (°C)	Duration
1	Initial denaturation	98	30 s
2	Denaturation	98	5 s
3	Annealing	Primer specific Tm	30 s
4	Elongation	72	20 s per 1 kb
5	Return to step 2 (32x)		
6	Final elongation	72	2 min

4.1.3. Restriction enzyme digestion of plasmids and PCR products

Plasmid DNA or purified PCR products were digested with suitable restriction enzymes for molecular cloning purposes. Restriction enzymes from NEB (USA) were preferred and digestion reactions were carried out according to manufacturer's instructions using the appropriate digestion buffers and temperatures, specific for each restriction enzyme.

4.1.4. Agarose gel electrophoresis

DNA fragments were run on agarose gels for diagnostic purposes and agarose gel extraction procedure. For routine applications, 1% agarose gel was employed. In order to differentiate large DNA fragments between 5-10 kb, low % agarose gels (0.7%); for small DNA fragments (50-200 bp), high % agarose gels (2%) were used. 400 ml of 1% agarose gel stock solution was prepared from 4 g agarose resuspended in 400 ml of 1X TAE buffer. The stock solution was boiled in a microwave until the agarose was completely dissolved. For one mini-agarose gel, around 50 ml of stock solution was mixed with 3 μl of EtBr under fume hood. The rest of the stock solution was kept in 65 °C oven until later use. DNA samples were run in 1X TAE buffer containing gel electrophoresis tanks. DNA Gel Loading Dye (6X) was used in all experiments as the loading dye.

4.1.5. PCR purification and agarose gel extraction

PCR products and restriction enzyme digested DNA fragments were purified with spin columns using the PCR purification kit according to manufacturer's instructions (High Pure PCR Purification Kit, Roche, Switzerland), when the PCR products or the digested DNA fragments were composed of one type of DNA fragment. Primer dimers or other small DNA fragments smaller than 100 bp do not efficiently bind to spin columns, so that DNA fragment of interest can be purified from small DNA fragments using PCR purification method. In other cases, where there are several DNA fragments larger than 100 bp, the DNA sample was run on agarose gel and the DNA fragment

of interest was cut using a razor under UV light. The DNA was extracted using the agarose gel extraction protocol according to manufacturer's instructions (High Pure PCR Purification Kit, Roche, Switzerland).

4.1.6. Ligation of DNA fragments

Restriction enzyme digested plasmid vectors and inserts were ligated using T4 polymerase (NEB, USA). In all ligation reactions, vector and insert concentrations were adjusted in a way that 1:3, 1:5, 1:7 (vector : insert) ratio. In each ligation reaction 10-30 ng of vector and corresponding amount of insert DNA were added, without exceeding the threshold of 100 ng (vector+insert) per 10 μl ligation reaction.

For example, in order to ligate 4000 bp vector and 1000bp insert, 20 ng of vector and (20 X 5) / 4 = 25ng of insert were added to ligation reaction. 1 μl of 10X ligation buffer and 0.5 μl T4 ligase were added and reaction was added up to 10 μl using ddH20. It is important to aliquot 10X ligation buffer for single use only since repeated freeze-thawing destroys ATP which decreases ligation efficiency.

4.1.7. Transformation of plasmids into competent bacteria strains

The ligated DNA fragments or plasmids were transformed into competent bacterial strains. For molecular cloning and re-transformation purposes, Top10, Stbl3, Rosetta strain of E. Coli was used. Top10 strain does produce enzymes that methylate plasmid DNA.

Half of the ligation reactions or 1-2 ng of plasmid to be re-transformed were added on top of the Top10 strain competent cell aliquots. Competent cells + DNA were incubated on ice for 20 minutes and then incubated at 42 °C for 40 s in water bath (heat shock). 100 μl of antibiotic-free LB was added on competent cells and incubated at 37 °C at rocking agitation (recovery). Finally, cells were plated on pre-warmed LB-agar plates including suitable antibiotics and incubated at 37 °C for 16 h.

4.1.8. Colony PCR

16 h after ligation products were transformed into competent cells, colony PCR procedure were executed to screen for positive colonies. Briefly, 20 μl +1μl of ddH20 was aliquoted into 8-strip PCR tubes. One backup plate with suitable antibiotics was marked with grids and numbered. With sterile micropipette tips, colonies were sampled, dissolved in the PCR tubes, additional 1μl ddH2O containing colony is dropped onto backup plate. Bacterial samples in ddH20 were incubated at 95 °C for 15 minutes (lysis). Then, PCR mixtures were added on top (Table 4.2) and the PCR reaction was executed (Table 4.3). Primer pairs used in colony PCR reaction were chosen in a way that the size of the resulting band can be differentiated from negative colonies (empty vector plasmid containing). Ideally, one of the primers anneals to the vector and the second primer anneals to the insert so that only the recombinant, newly synthesized construct is able to give the correct band.

Table 4.2. PCR mixture for the colony PCR reaction.

Reagent	Initial concentration	Volume(μl)
Buffer	10X	3
MgCl2	50mM	1.05
dNTP	10mM	0.6
Forward primer	10 pmole/μl	1.5
Reverse primer	10 pmole/μl	1.5
Template		+
Taq		1
ddH20		20 + 1.35
Total		30

Table 4.3. PCR protocol for the colony PCR reaction.

Step #	Description	Temperature (°C)	Duration
1	Initial denaturation	95	30 s
2	Denaturation	95	5 s
3	Annealing	Primer specific Tm	30 s
4	Elongation	72	60 s per 1 kb
5	Return to step 2 (32x)		
6	Final elongation	72	5 min

4.1.9. Analytic digestion (Diagnostic digestion)

Positive colonies identified with the colony PCR procedure were screened via analytical digestion reactions. Briefly, positive colonies were picked with a sterile tip from the backup plate and put into LB with the suitable antibiotics (liquid bacterial culture). Bacteria were grown at 37 °C for 16 h with rocking agitation. Mini-scale DNA isolation was executed as in Section 4.1.1. Subsequently, isolated plasmid DNA was digested as in 4.1.3 using a restriction enzyme pair that gives rise to a pattern that can be distinguished from negative colonies (empty vector plasmid containing).

4.1.10. Sequencing of plasmid constructs

Each construct used in this study was checked using Sanger sequencing. Sequencing service was purchased from Macrogen Europe, Amsterdam the Netherlands.

4.2. Cloning strategies

4.2.1. pEGFP-C3-H5 plasmid

In order to create a plasmid encoding a fusion protein of EGFP and H5, cDNA of H5 was obtained by PCR from pBBSK-H5 plasmid. Using the designed forward and reverse primers having HindIII restriction enzyme, H5 insert is produced. pEGFP-C3 plasmid and the PCR product are digested with the same enzyme;HindIII. In order to prevent re-ligation of this plasmid, alkhaline phosphatase treatment is done. Vector and insert fragments were purified as in Section 4.1.5 and ligated as in Section 4.1.7. Colonies were screened via colony PCR using the GFP-F and H5-R primer pair as in Section 4.1.9. Positive colonies were further analyzed using diagnostic digestion using the HindIII enzyme as in Section 4.1.10. Colonies were further checked using Sanger sequencing using CMV-F and H5-R primers.

4.2.2. pet30a+H5

In order to create a plasmid encoding a fusion protein of His tag and H5, cDNA of H5 was obtained by PCR from pBBSK-H5 plasmid. Using the designed forward and reverse primers having HindIII restriction enzyme, H5 insert is produced. pet30a+ plasmid and the PCR product are digested with the same enzyme;HindIII. In order to prevent re-ligation of this plasmid, alkhaline phosphatase treatment is done. Vector and insert fragments were purified as in Section 4.1.5 and ligated as in Section 4.1.7. Colonies were screened via colony PCR using the CMV-F and H5-R primer pair as in Section 4.1.9. Positive colonies were further analyzed using diagnostic digestion using the HindIII enzyme as in Section 4.1.10. Colonies were further checked using Sanger sequencing using CMV-F and H5-R primers.

4.2.3. pcDNA3-H5(69-133)-ASC

In order to create a plasmid encoding a fusion protein of H5 and ASC, cDNA of H5 was obtained by PCR from pBBSK-H5 plasmid. Using the designed forward and

reverse primers having HindIII restriction enzyme, H5 insert is produced. pcDNA3-hASC plasmid and the PCR product are digested with the same enzyme;HindIII. In order to prevent re-ligation of this plasmid, alkhaline phosphatase treatment is done. Vector and insert fragments were purified as in Section 4.1.5 and ligated as in Section 4.1.7. Colonies were screened via colony PCR using the CMV-F and H5-R primer pair as in Section 4.1.9. Positive colonies were further analyzed using diagnostic digestion using the HindIII enzyme as in Section 4.1.10. Colonies were further checked using Sanger sequencing using CMV-F & H5-R primers and CMV-F & reverse primer designed inside ASC.

4.3. Western blotting analysis

4.3.1. Preparation of samples

Cell culture samples were collected in lysis buffer (Table 3.9) using a scraper. Typically, 200 μl of lysis buffer was added on a well of 6-well plate (106 cells) and cells were collected. Subsequently, samples were sonicated via executing the sonication program for 3 times (5 seconds, 3 cycles, 50%power) on ice in 15 ml falcon tubes. Subsequently, tubes were briefly spinned down at low speed to collect droplets on the walls. Samples were transferred into 1.5 ml tubes and 40 μl 6X Laemli buffer (Table 3.9) was added. Samples were denatured at 95 °C for 5 minutes, and stored at -20 °C until later use.

4.3.2. Preperation of SDS-PAGE gels

For routine use, 0.75mm 15-well SDS-PAGE gels were casted. Briefly, liquid 15%gel solution (4 ml per gel) was mixed with 40 μl 10% APS and 4 μl TEMED (resolving gel). The gel solution was mixed thoroughly and put between casting glasses. The gel was immediately covered with isopropanol to ensure a flat surface. Once the resolving gel was polymerized (around 30 minutes), isopropanol was drained off. Stacking gel mixture was prepared. 1 ml per gel 4% gel solution was mixed with 10 μl 10% APS and 1 μl TEMED. The mixture was added on top of the resolving gel and

the comb was inserted. After polymerization was completed, the gel was wrapped with tissue paper and wetted with ddH20, put in a plastic bag and kept at 4 °C until later use, for no longer than 1 week.

4.3.3. Protein Gel Electrophoresis

The SDS-PAGE gels were run in vertical electrophoresis tanks in 1X TGS buffer. Prior to electrophoresis, samples were briefly incubated at 95 °C for 2 minutes and vortexed. 10 μl of sample were loaded to each well in 0.75mm 15-well SDS-PAGE gels. Empty wells were loaded with blank sample (PBS mixed with 6X laemli) to avoid "smile effect". Samples were run at 80 V until they enter resolving gel, then the voltage was increased to 130 V. The gel electrophoresis was stopped as the dye front reached the end of the gel.

4.3.4. Semi-dry transfer

Proteins in the SDS-PAGE gels were transferred onto nitrocellulose membranes using the semi-dry transfer method. Briefly, a sandwich of 2 filter papers, SDS-PAGE gel, nitrocellulose membrane and 2 filter papers was prepared on the semi-dry transfer apparatus. Bubbles between sandwich layers were removed with a falcon tube used as a roller. Cover of the transfer apparatus is closed with the correct orientation (the proteins run towards positive pole). The transfer was completed at 10 V for 35min.

4.3.5. Membrane blocking

The nitrocellulose membrane was taken into a plastic tank for subsequent incubations with the protein side facing upwards. The membrane was washed for 5 minutes with TBS-T and blocked with 5% BSA for 1 h at RT. After blocking, the membrane was washed for 5 minutes with TBS-T.

4.3.6. Antibody incubations

The membranes were incubated with the primary antibody solutions at 4 °C overnight. Sodium azide was added into the primary antibody solution to inhibit microbial growth. When the incubation was finished, the primary antibody was stored at 4 °C for repeated usage. The membrane was washed 3 times after primary antibody incubation with TBS-T, then incubated with a secondary antibody solution at RT for 1 hour. Sodium azide was not included into secondary antibody solution, as it inhibits HRP on the secondary antibody. The secondary antibody was chosen according to the animal in which primary antibody was raised (mouse in our study). After secondary antibody incubation, the membrane was washed 3 times with TBS-T.

4.3.7. Visualization of the membrane

The color reagents were mixed with one-to-one ratio and added on the membrane which was placed on a clean glass surface (Stella). Bubbles were removed. The imaging was conducted using a digital visualization device (Stella, Raytest, Germany).

4.4. Confocal analysis

4.4.1. Seeding cells on coverslips

The confocal microscope used in this study is an upright microscope. Therefore, cells need to be plated onto coverslips and inverted by putting onto a glass slide. For this purpose, glass coverslips were put on 6-well plates and treated under UV for at least 1 h. HEK293T or THP-1 cells were plated on coverglass containing wells afterwards.

4.4.2. PFA fixation

Cells were fixed in 4% PFA solution at room temperature for 5 minutes. PFA was then removed and cells were kept in PBS and stored in dark at 4 °C until analysis.

4.4.3. DAPI staining

1 mg/ml (200X) DAPI stock solution was aliquoted and stored in -20 °C. The stock solution was diluted in PBS to 1X concentration. 1X DAPI solution was added dropwise on fixed cells attached to the coverslips. Cells were incubated at RT for at least 5 minutes. Subsequently, the wells were washed once with PBS.

4.4.4. Immunocytochemical staining

Remove fixative by washing the slides 3x 10 min with 1XPBS. Permeabilize and block cells with blocking solution-2 (0.25 %Trt X-100/0,25 % BSA/1x PBS) for 30 min. OPTIONAL: Wash 2x 5 min with the washing solution (0.25 % Trt X-100/1X PBS). Incubate cells O/N with the primary antibody diluted in blocking solution-2 at 4 °C (or 1 hour at room temp). Rinse 3x 10 min with washing solution. Incubate cells with the secondary antibody in blocking sol-2 for 1 h at dark. Incubate with 0.02 μg/ml (20 μM) DAPI in 1X TBS for 5 min. Rinse 3x 10 min with PBS/washing solution. Put mounting medium. Store at 4°C, at dark.

4.4.5. Visualization by the confocal microscope

Fluorochromes were excited using appropriate wavelengths and the emitted photons were scanned using the ranges given in Table 4.4.

Table 4.4. Excitation and emission wavelengths used in confocal microscopy analysis.

Fluorochrome	Laser	Excitation (nm)	Emission range (nm)
DAPI	Diode, 50 mW	405	410-450
EGFP	Ar, 65 mW	488	490-535
mCherry	HeNe, 1 mW	543	570-680

4.5. Cell culture

4.5.1. Maintainance of THP-1 cells

THP-1 is an established monocytic cell line derived from a leukemia patient. The cell line displays macrophage-like characteristics upon differentiation with PMA. Undifferentiated THP-1 cells were cultured in suspension with RPMI supplemented with supplemented with 1x MEM Non-Essential Aminoacids, 2mM L-Glutamine, 100 U/ml penicillin, 100 μg/ml streptomycin and 10% FBS. THP-1 cells were not allowed to exceed the maximum confluency of 1×10^6 per 1 ml. Freezing of THP-1 cells was carried out in 50% FBS and 5% DMSO containing full RPMI medium. Aliquots of THP-1 cells were stored at -150 °C indefinitely in the freezing media using cryotubes. Frozen vials were thawed using a water bath at 37 °C. Freezing media were changed with full RPMI medium supplemented with 20% FBS. Cultures were maintained in 20% FBS containing RPMI until cells acquired their normal morphology.

4.5.2. PMA differentiation of THP-1 cells

5×10^6 THP-1 cells were differentiated in 60 mm plates in 0.5 μM PMA containing RPMI for 3 h. Subsequently, cells were collected by scraping. Cells were incubated for 24 h in PMA-free RPMI.

4.5.3. Bone marrow derived dendritic cell isolation and maintenance

Dendritic cells are isolated from the bone marrow of C57/BL6 mice. Tissue free femur bones are sterilized with 70% EtOH. From the cutted edges of the bones, FBS is flushed away with 27G needle syringe onto 50μm cell strainer to have the dendritic cells inside the bone. With the help of plunger of a syringe, marrow was excluded from the strainer into falcon. 1ml RBC lysis buffer is used to remove RBCs. 20ng/ml GM-CSF is added to culture to led only the dendritic cell population survival. BMDCs were cultured in suspension with RPMI supplemented with supplemented with 100 U/ml penicillin, 100 μg/ml streptomycin, 10% heat-inactivated FBS, 5 ml HEPES,

and 50μM 2-mercaptoethanol.

4.5.4. Maintainance of EG.7/EL4(OVA) cells

EG.7-OVA cells (ATCC, USA) The EL4 cells were transfected by electroporation with the plasmid pAc-neo-OVA which carries a complete copy of chicken ovalbumin (OVA) mRNA and the neomycin (G418) resistance gene. E.G7-OVA cells contain a single copy of the inserted plasmid and synthesize and secrete OVA constitutively. C57BL/6 mice immunized with E.G7-OVA cells give rise to H-2 Kb restricted cytotoxic lymphocytes specific for the OVA 258-276 peptide. EG.7-OVA cells were cultured with RPMI 1640 medium with 2 mM L-glutamine adjusted to contain 1.5 g/L sodium bicarbonate, 4.5 g/L glucose, 10 mM HEPES and 1.0 mM sodium pyruvate and supplemented with 0.05 mM 2-mercaptoethanol and 1 mg/ml G418 (once a month), 90%; fetal bovine serum, 10%.

4.5.5. Maintainance of HEK293T cells

HEK293(F)T cells (Invitrogen, USA) are widely used for protein overexpression and lentiviral packaging purposes. These cells were derived from HEK293F cells which stably express the SV40 large T antigen from the pCMVSPORT6TAg.neo plasmid. HEK293T cells were cultured with high glucose DMEM supplemented with supplemented with 1x MEM Non-Essential Aminoacids, 2mM L-Glutamine, 100 U/ml penicillin, 100 μg/ml streptomycin and 10% FBS.

4.5.6. Calcium Phosphate Transfection

HEK293T cells were efficiently transfected via the calcium phosphate transfection method. This procedure produces insoluble precipitates of plasmid DNA and calcium phosphate, which are subsequently engulfed by HEK293T cells. Briefly, plasmid DNA to be transfected were mixed with ddH20, 2M CaCl2 and 2X HBS solution in the given order, with the amounts indicated at Table 4.5. Incubation time after CaCl2 and 2XHBS addition does change size of the calcium-phosphate-DNA co-precipitates

which affects transfection efficiency. The incubation time is determined empirically as 5 minutes after addition of CaCl2 and 2XHBS. Vortexing the transfection mixture should be avoided as it decreases transfection efficiency. However, it is recommended to mix the solution after 2XHBS addition till bubbles are observed.

Table 4.5. Preparation of transfection reagents for calcium phosphate transfection.

	DNA	**d**dH20 (add up to)	**2**M CaCl2	2XHBS
6-well plate	0.5-1 μg	219 μl	30.5 μl	250μl
100 mm dish	4 μg	439 μl	61 μl	500 μl
150 mm dish	12 μg	1317 μl	183 μl	1500 μl

4.6. Purification of ASC specks from HEK293T cells

4.6.1. Crude extraction

Transfection of ASC encoding plasmids was carried out via calcium phosphate method as in Section 4.5.5. Cells were collected 24 h after transfection by scraping in 3 ml PBS for each 150mm dish. Cells were combined in 50 ml falcon tube and sonication program was run for 5 times, 5 seconds 3x10%, 50% power program in ice. The lysate was centrifuged at 200 g at RT for 5 minutes in Beckmann falcon centrifuge. Due to micrometer size of the ASC specks, they were found in the low speed centrifugation pellet. Soluble proteins remained in the supernatant which was discarded.

4.6.2. High purity isolation of ASC specks

Transfection of ASC encoding plasmids was carried out via calcium phosphate method as in Section 4.5.5. Cells were collected 24 h after transfection by scraping in 3 ml PBS for each 150mm dish. Lysates of 3x150mm dishes were combined in a 50 ml falcon tube. Sonication program was run for 5 times, 5 seconds 3x10%, 50% power program in ice. The lysate was centrifuged at 2400 g for 5 minutes at RT

in Beckmann falcon centrifuge. The pellet was resuspended by vigorous vortexing. After complete resuspension, lysates were left to gravity sediment for 5 minutes. The first gravity sedimenting filamentous pellet was observed to be rich in nucleic acids and granular proteins but deficient in ASC protein (shown by Ali Can Sahillioğlu). Taking advantage of this observation, this cycle was repeated until sufficient purity was achieved. Upon gravity sedimentation, the supernatant was transferred into a new falcon tube. The supernatant was centrifuged at 200 g for 5 minutes at RT in Beckmann falcon centrifuge. The supernatant was discarded and pellet was resuspended in 10 ml PBS. The pellet was resuspended by vigorous vortexing. The lysate was left for gravity sedimentation for 5 minutes and the supernatant was carefully saved. The supernatant was centrifuged for 60 minutes at 200 g at RT. The pellet was resuspended on 30 ml PBS.

After sequential gravity sedimentation, granular particles smaller than ASC specks were removed by first passing the sample through a 5 μm syringe filter and then re-applying PBS in the opposite direction (reverse flow). By this method, not only ASC specks greater than 5 μm but smaller specks were recovered as well, possibly due to uneven size distribution of the filter. 30 ml sample was passed from the syringe filter in 6 cycles and at the end of each cycle reverse flow was applied. Sequential passing of the sample is necessary not to clog the filter. Finally, the sample was centrifuged at 2400 g for 60 minutes. The pellet was resuspended in 0.5 ml PBS. The typical yield of this method is around 100-200 μg of ASC specks per 5×10^7 HEK293T cells. It is important not to centrifuge ASC specks at high speed (ex. 20 000 g) as high speed centrifugation pellets could not be resuspended.

4.7. Expression and purification of H5 from E.Coli

pETM-30a+H5 plasmid was transformed into Rosetta2 pLysS strain of E. Coli as in Section 4.1.8. Transformed bacteria were plated on ampicillin and chloroamphenicol containing LB-agar plates. A single colony was picked and cultured in ampicillin and chloroamphenicol containing 20 ml LB starter culture. Next day, 20 ml of the starter culture was added on 1 L ampicillin and chloroamphenicol terrific broth. The culture

was shaked for about 3 hours at 37 °C until the OD reached 0.85. At this time point, 1 ml of 1 M IPTG (1 mM final concentration) was added on 1L culture and shaked 2 hours at 37 °C. Then, culture was splitted into 2x50 ml falcon tubes. The pellet was resuspended in 5 ml equilibration buffer (PBS + 50mM imidazole). The His-TRAP Column was equilibrated with equilibration buffer. The lysate was then applied to the column in 5ml aliquots. The column was washed for 3 times with wash buffer (PBS + 50mM imidazole). The column was eluted for 3 times with elution buffer (PBS + 200 mM imidazole). The sample was dialyzed against PBS at 4 °C overnight. The purity of the sample was monitored by SDS-PAGE and Coomassie staining and the concentration was measured by Bradford assay.

4.8. Immunizations

50 μg OVA-ASC, OVA-Freund's adjuvant, OVA-PBS & H5-ASC, H5-Freund's adjuvant, H5-PBS protein injections are done i.p. to C57/BL6 mice (4 mice/sample). Injections are done 3 times within 2 week intervals. before every injection, blood sampling is done. 2 days after the final boost, blood sampling is done. Mice sera is aliquoted and stored at -80°C till usage. In order to check antigen specific IgG titers, ELISA is done with those sera.

4.8.1. Injections of antigen loaded ASC specks for IVIS

50 μg of mCherry-ASC specks were injected subcutaneously, intraperiotanelly, intraveniously to 3(three) C57/BL6 mice for *in vivo* imaging. 50 μg of H5-ASC, OVA-ASC specks and H5/ OVA/ H5-Freund's adjuvant/ OVA-Freund's adjuvants proteins were injected intraperiotanelly to 4(four) C57/BL6 mice per each sample. mCherry-ASC specks were purified as in Section 4.6.2 and H5 protein was purified from Rosetta as in Section 4.7.1. Mice were anesthetized during procedure with ether.

4.8.2. IVIS analysis

For our experiment we used the IVIS Spectrum *in vivo* imaging system uses a back-thinned charge coupled device cooled to -90°C to achieve maximum sensitivity. To support absolute quantitation, the system measures dark charge during down-time and runs a self-calibration during initialization. We selected field of view for three number of animals being imaged in the instrument using the integral anesthetic manifold. The stage is at a constant 37°C to maintain body temperature in the animals. Representative fluorescence reflectance images (excitation filter, 587 nm and emission filter, 610 nm) of mice injected i.p.,i.v.,s.c. with mCherry fluorescent protein tagged ASC specks. Scale bar, 1 cm. The color bar indicates radiant efficiency $\times 10^6$; minimum is 0.001, and maximum is 0.006. Fluorescence data were reported as signal-to-noise ratio (Signal/Bkg), where background fluorescence was measured from the same mouse nearby the injection site.

4.8.3. ELISA

For ELISA experiments, 96 well plates are coated with ovalbumin or H5 day before the experiment at RT. Next day, after blocking with BSA, 1:100 diluted mice sera is added and incubated 2 hours at RT. After that as 1:2000 diluted secondary HRP-conjugated mouse IgG is added and incubated 2 hours at RT. Substrate solution is added to each well for 20 minutes at RT. Finally, stop solution was added to samples and optical density of the samples was detected by substracting the readings at 530nm from reading at 450nm. Triple well is used per sample. Standart curve is graphed by using commercial ovalbumin and H5 proteins. Finally, animals were sacrificed and spleens were removed.

4.8.4. *In vitro* FACS experiments

Spleens were put into RPMI. Using a 40 μm cell strainer, splenocytes were obtained by squashing the spleen with a back of syringe. 1ml ACK lysis buffer(5min at RT) addition eliminated the red blood cells. We filled the cells and lysis buffer

containing 50ml falcon with complete medium, spinned them for 6min at 1500rpm, resuspended them in 10ml complete medium. Then FACS staining was done with the antibodies in correct dilutions in FACS buffer, 30 min incubation on ice at dark, washing steps, and the analysis was done afterwords.

5. RESULTS

5.1. Efficient phagocytosis of ASC specks by primary mouse BMDCs

Immunization is achieved if the vaccine antigens are engulfed by APCs. Sahillioğlu A. in our laboratory previously showed that ASC specks are engulfed by differentiated THP-1 macrophages. In this experiment, we wanted to show that dendritic cells, which are one of the most important targets of vaccination, are able to engulf antigen loaded ASC specks.

p(delta 1-235)OVA-ASC plasmid (by Ali Can Sahillioğlu) was used for HEK293T transfection for OVA-ASC production. At day 8 after BMDC isolation, cells were seeded into 6 well plates. OVA-ASC specks purified from HEK293T cells were incubated with dendritic cells for 36 hours at 37°C- 5% CO2. After fixation of DCs with 4% PFA, immunocytochemical staining was done with anti-ASC antibody which is detected with Goat Anti-Mouse Alexa Fluor® 488 antibody (488nm excitation), thus giving green color. The nucleus was stained with DAPI(405nm excitation), giving blue color.

Using confocal microscopy, we have shown that cells identified with DAPI give green fluorescence coming from ASC specks inside the cell.

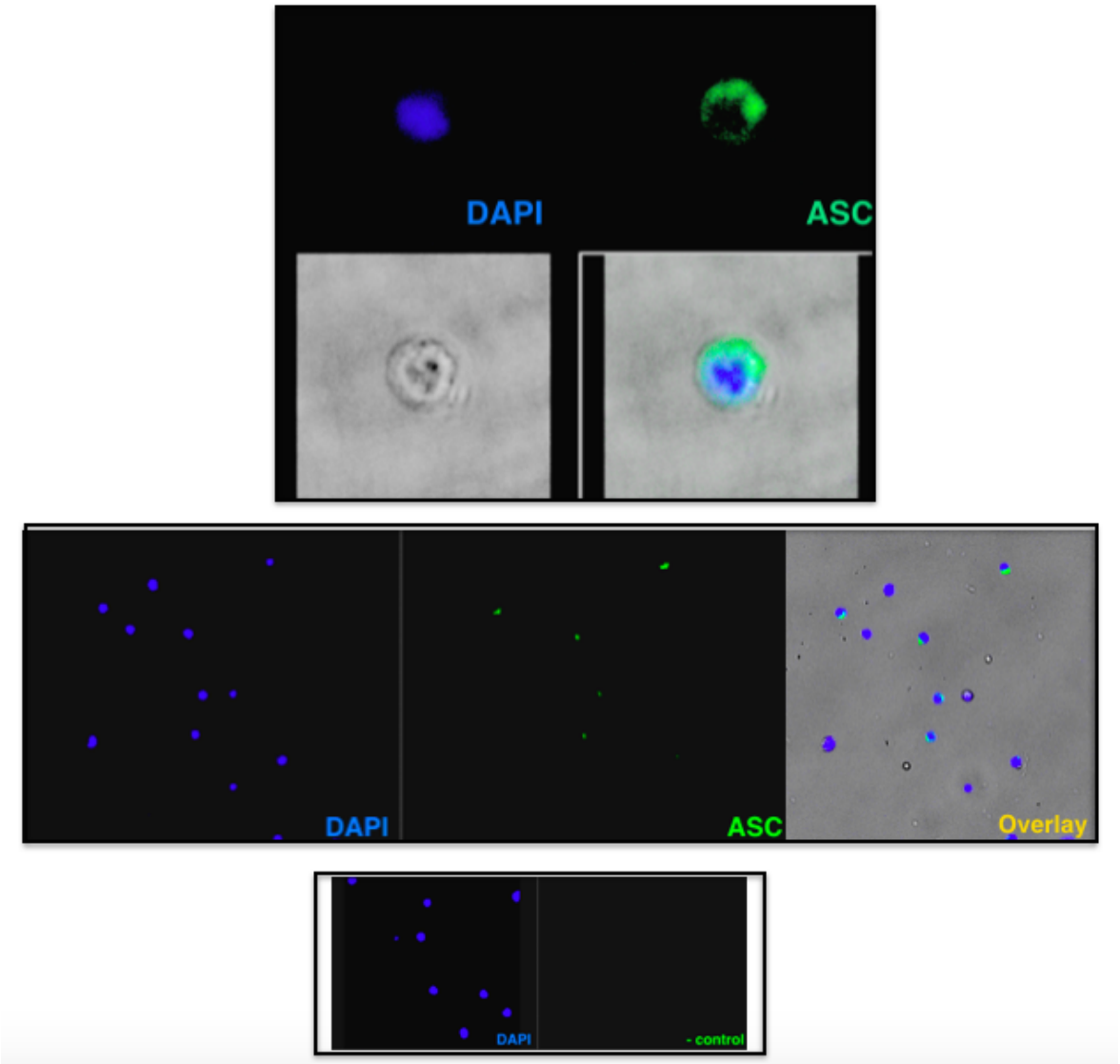

Figure 5.1. BMDCs are able to engulf ASC speck containing antigen ovalbumin.

5.2. Medium scale production and purification of OVA loaded ASC specks and mCherry tagged ASC specks for *in vivo* studies

In order to initiate immunization studies in C57/BL6 mice, we needed at least 50μg purified protein per injection. Since we have to repeat the experiments and 4 mice per sample, we needed to do medium scale production of OVA-ASC and mCherry-ASC proteins. To do so, totally we used 50x 150 cm tissue culture dishes for HEK293T cell

transfection per sample.

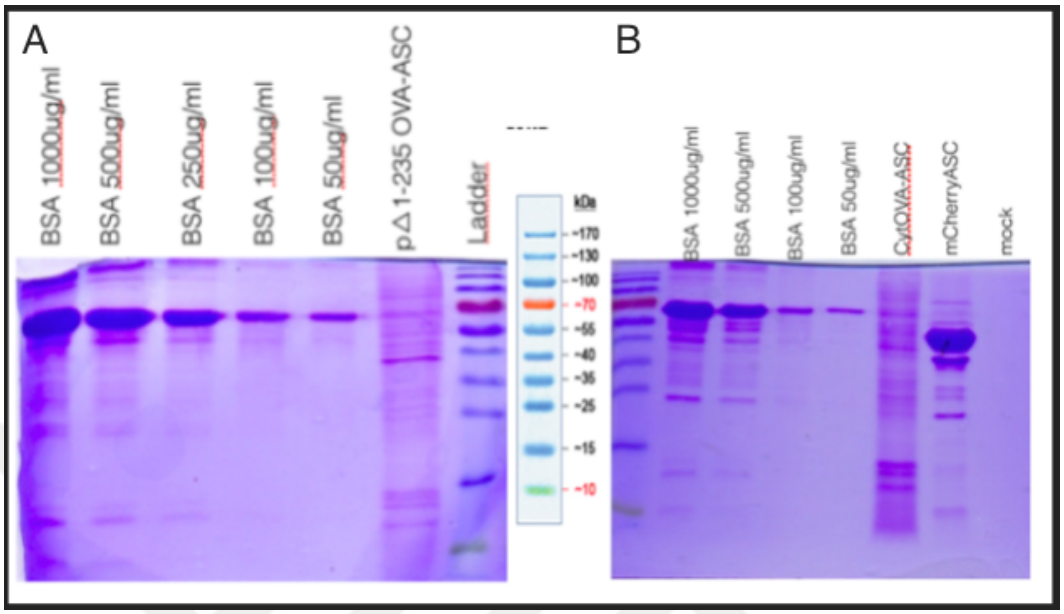

Figure 5.2. Purified antigen fused specks from HEK293T cell line. A) OVA-ASC, B) mCherry-ASC specks were purified. Purified specks were run side by side with BSA standards for concentration determination. Gels were stained with Coomassie blue.

At the end, we finally had sufficient amount of protein production from HEK293T cell line and purified them with ASC speck purification protocol. Total yield was 500μg OVA-ASC, 100μg mCherry-ASC.

5.3. Distribution of injected ASC specks in animal tissues

Increasing the duration of antigen presentation has high importance to trigger immunity. Particulate antigen delivery systems are used for this purpose, as they can prolong the antigen's stability. We designed an *in vivo* experiment to track the distribution and check the stability of our purposed antigen delivery system. We injected 50 μg mCherry labelled ASC specks subcutaneously, intraperitoneally and intravenously into 3 different mice. As a control, we injected 1X PBS via the same routes. We observed fluorescent intensity using IVIS live imaging system. 3 hours after the s.c.,

i.p., i.v. injections, we proof that we can visualize the specks under IVIS [Figure 5.3].

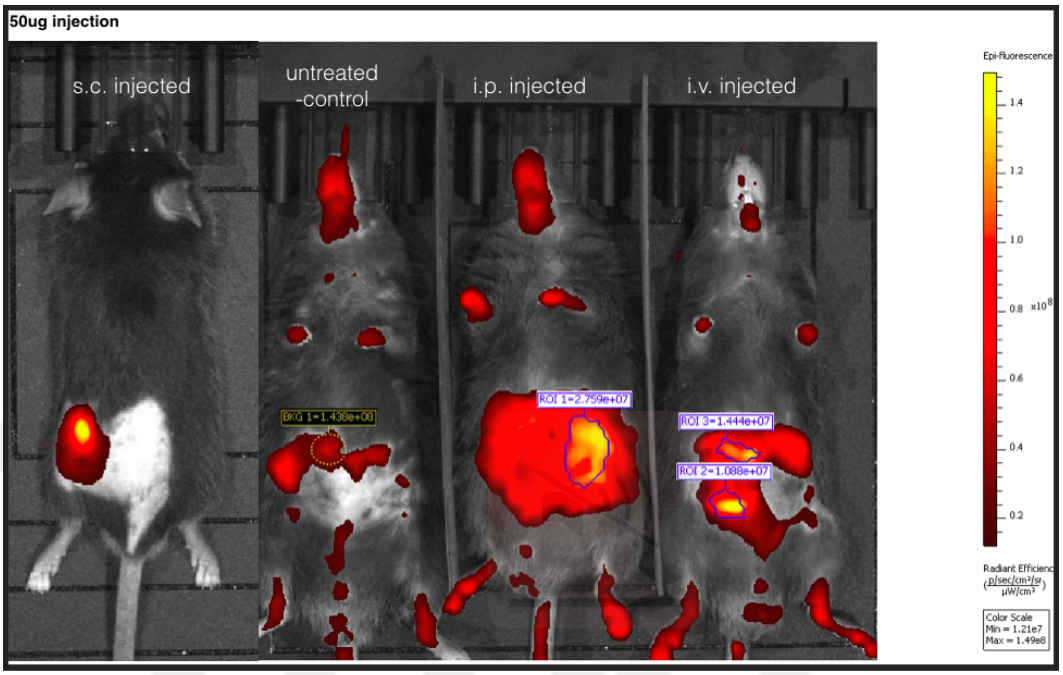

Figure 5.3. Visualization of ASC specks inside mice body.

Initially the red fluorescence was dispersed in the abdominal cavity in the i.p.&i.v. injected animals. We noticed that at day 7, ASC specks are localized in the spleen. At day 14, they went through the lymph nodes of the gut [Figure 5.4]. Thus, we showed for the first time that at least they can stay 2 weeks inside the mice body. After a month specks are degraded and eliminated from the body. We concluded that coupling of mCherry to the ASC speck increases its persistence in the system.

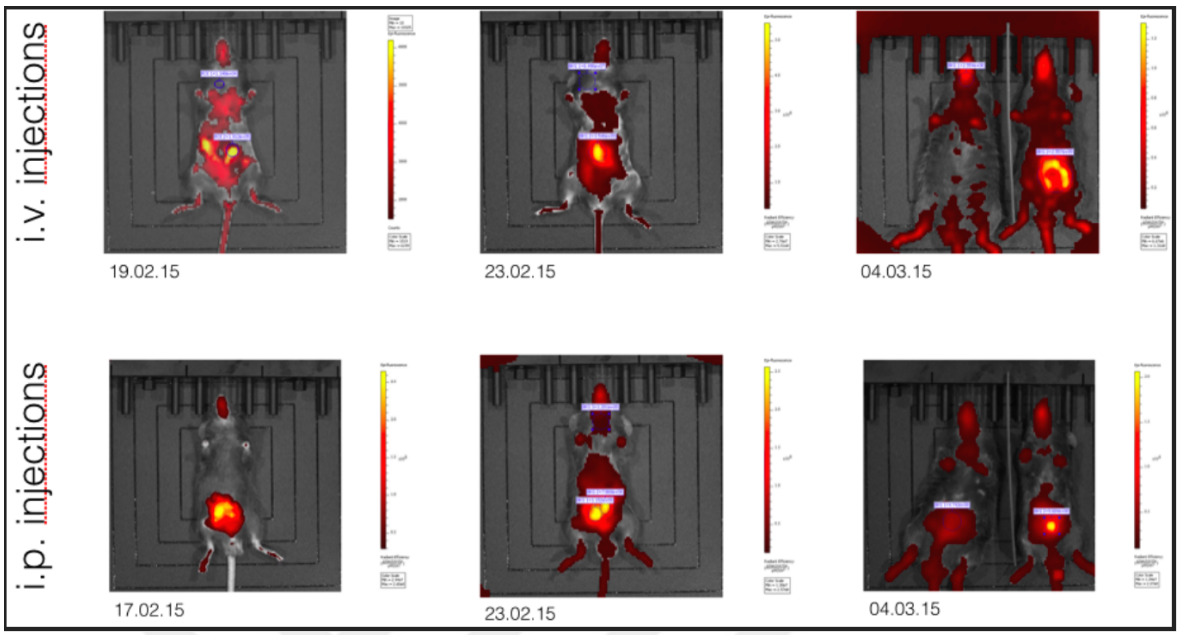

Figure 5.4. Stability of ASC specks inside mice body continues for 3 weeks.

5.3.1. ASC specks localize to the spleen for three weeks.

It is known that after an infection, immune cells (originated in bone marrow) such as macrophages and dendritic cells bind to the antigen which promotes immune cell maturation in secondary lymph node. In the lymph nodes and spleen helper T cells & B cells become activated. Vaccination mechanisms work in the same way. Thus, the antigen arrival to the central immune organ "spleen" is really important for any vaccine to be effective. In order to prove that ASC specks can infiltrate into the spleen, we sacrificed the mCherryASC vaccinated mice and dissected the spleens for visualization under IVIS. We demonstrated that mCherry-ASC i.p. vaccinated mice have ASC specks in the spleen 3 weeks post injection [Figure 5.5].

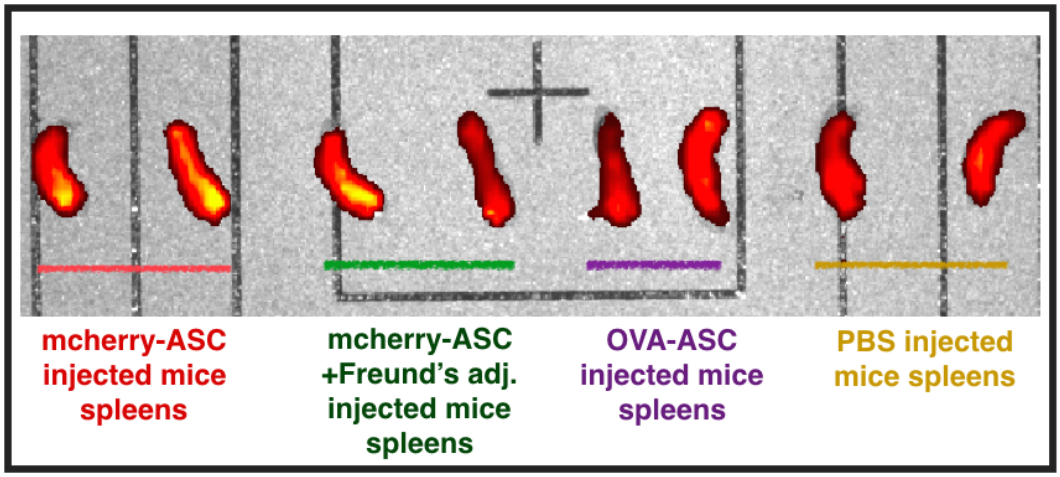

Figure 5.5. Injected mCherry-ASC specks localized to spleen 3 weeks after i.p. injection when compared to non-fluorescent tagged speck injected mice spleens.

5.4. Detection of OVA specific humoral immune responces

In vivo studies are necessary to demonstrate the effectivity of a novel antigen carrier, such as the ASC specks. Thus, we designed experiments to immunize mice with the produced antigen loaded ASC specks.

5.4.1. OVA-ASC fusion speck immunzations lead to increase in OVA specific IgG titers

As a preliminary work, we used 10 μg OVA-ASC and PBS injections to see the ovalbumin specific IgG production. Immunization was done 3 times with 2 week intervals. Sampled blood sera was used for ELISA test. It is shown that OVA-ASC injections lead to 25% increase in OVA specific IgG titers [Figure 5.6].

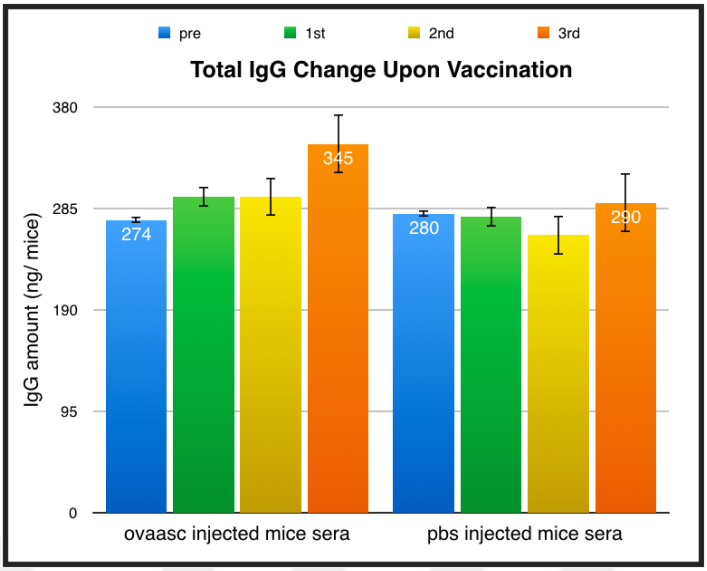

Figure 5.6. OVA-ASC i.p. injection promoted OVA specific IgG production.

Since we observed an OVA-specific IgG increase in the OVA-ASC injected mice sera, we designed immunization experiments in a larger number of animals with i.p. injection of 50μg antigen loaded ASC specks. 4 C57/BL6 mice were used per sample. OVA-ASC fusion protein, OVA-Freund's adjuvant mixture, OVA protein injections were done 3 times with 2 week intervals. (Freund's adjuvant is used as a positive control, only antigen injections are used as a negative control). OVA-ASC fusion speck injections lead to two fold increase in OVA specific IgG titers. [Figure 5.7] While there was about 100 ng OVA-specific IgG in unvaccinated mice sera, the IgG titers increased to about 700 ng after final boost with OVA-ASC fusion speck injections. In the positive control (OVA-Freund's complex injections), the IgG titers increased from 100 to 1600 ng after the final boost. As expected, there was no difference in mice injected with OVA protein itself which was used as a negative control.

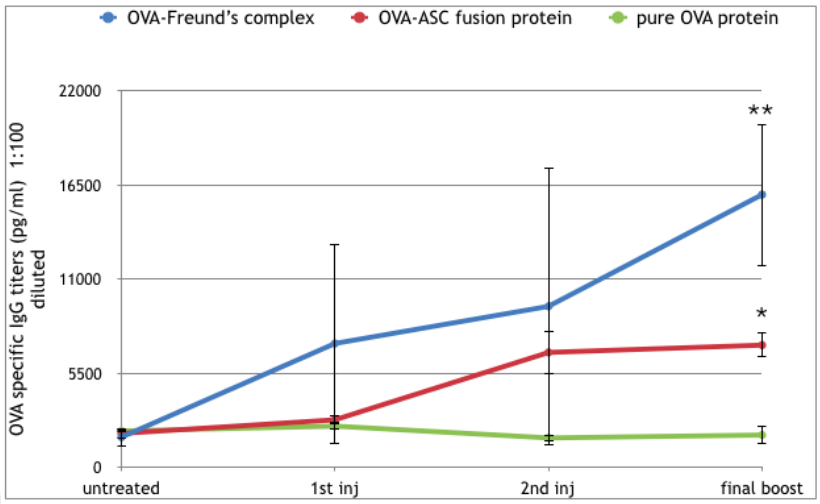

Figure 5.7. OVA-ASC injection significantly increased OVA specific IgG production.

In these experiments the total amount of injected protein was kept constant at 50μg. However, it should be noted that 50μg OVA-ASC fusion protein contains 1/2 OVA to 1/2 ASC. Thus, OVA amount was 1/2 of the OVA found in the pure OVA-Freund's.

5.4.2. ASC speck based immunization leads to changes in B&T cell populations of the spleen.

T cells interact with activated DCs and boast B cell responses. Most of the vaccines induce CD4+ T cell response which is important for CD8+ T cell and B cell differentiation. Adjuvants control the induction of CD4+ and CD8+ T cells [10]. Thus, we designed an experiment with splenocytes isolated from spleens of the vaccinated mice to compare B and T cell populations.

After the splenocytes were isolated, we did FACS staining of splenocytes with PE-conjugated CD4+ antibody, FITC-conjugated CD19 antibody, PE-conjugated B220 antibody (for total B-cell population), FITC-conjugated H57 antibody (for total T-cell population, C region of TCR β chain). We observed a significant increase in B cell

population of OVA-ASC vaccinated mice spleens with respect to control groups. OVA-ASC fusion specks injected mice had 43%, pure OVA injected mice had 37%, OVA-Freund's complex injected mice had 27% B cell population in their spleens. [Figure 5.8, Figure 5.9]

Interestingly, when we compared the B cell vs Mϕ populations within each different injection groups, we observed that decrease in Mϕ number increased the B cell number and vice versa. Especially, B cell population was maximum (%42,5) in OVA-ASC fusion speck injected groups and their Mϕ amount was the least (%63) compared to OVA-Freund's complex injected group (B cell %26,7; Mϕ %76).[Figure 5.8, Figure 5.9]

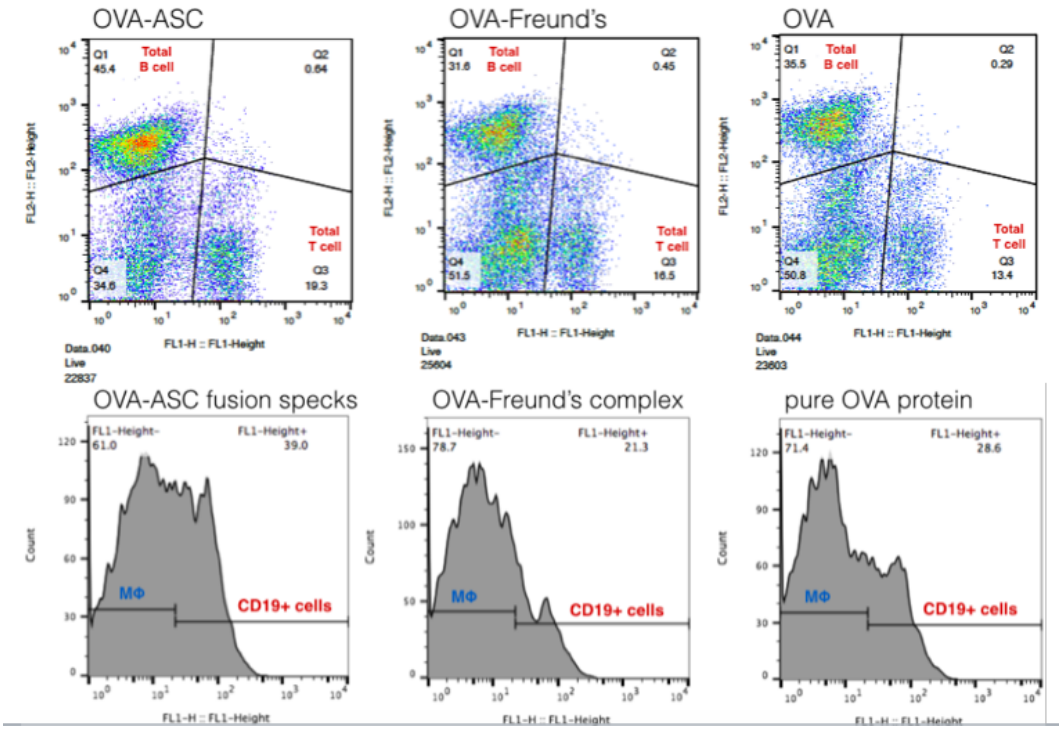

Figure 5.8. Cells were stained for cell surface CD4, B220, H57, CD19 expression and assessed by flow cytometry. One result per group is shown here.

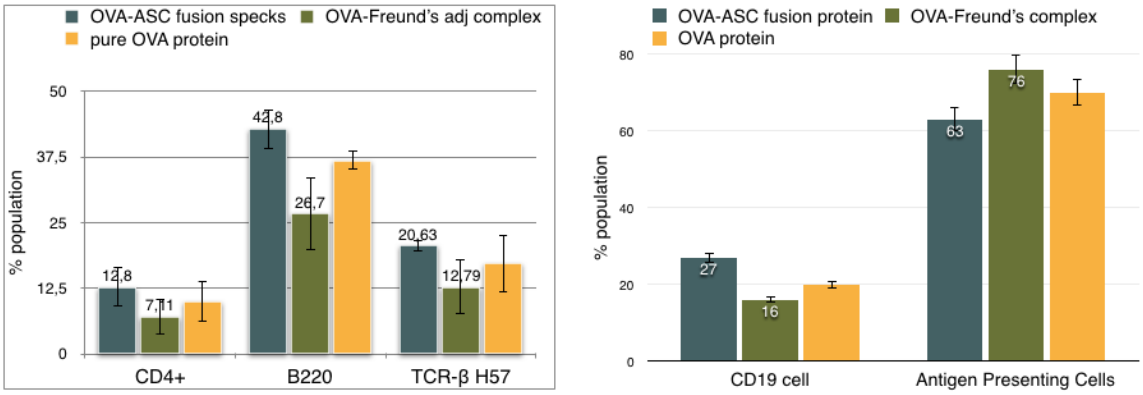

Figure 5.9. B cell population increased and macrophage population decreased in the spleen after mice immunization with OVA-ASC fusion specks. Cells were stained for cell surface CD4, B220, H57, CD19 expression and assessed by flow cytometry. Statistical comparison between groups was based on two-tailed unpaired Student's t test (n = 2 to 4).

Through these demonstrations we suggest that injected OVA-ASC fusion specks were engulfed by Mϕ and lead to activation of Mϕ and their own ASC specks formation, which follows the pyroptosis and extracellular release of ASC specks. This event continues likewise. Their significant decrease in cell number can be explained with this hypothesis. Increase in B cell population can be reconciled with Mϕ death, as activated Mϕ can secrete cytokines and after cell burst they release cytoplasmic proteins to the extracellular matrix needed to activate B&T cells which is followed by their proliferation.

5.5. ASC specks can be loaded with H5 antigen

We have previously shown that short peptides, several cytosolic proteins, hydrophobic peptides, and the model antigen ovalbumin co-aggregated on the ASC speck [13]. This suggest that the co-aggregation is not specific. In order to check whether this interesting observation can be applied to vaccination strategy, we carried out experiments to produce a prototype vaccine for H5N1 *H.Influenza*. First, we

checked the co-aggregation capacity of H5 onto ASC specks.

5.5.1. Cloning of H5 into pEGFP vector

We constructed a vector to test whether H5 can become part of ASC specks. H5 (1695 bp) was amplified with Q5 DNA Polymerase by using the designed primers. The plasmid used in this experiment is pcDNA3 (plasmid). Both the plasmid and the insert were digested with HindIII restriction enzyme. Ligation products were transformed into Stable3 competent E.Coli bacteria. Positive colonies were detected with CMV-F and H5-R primers in a colony PCR set up [Figure 5.10]. This construct is referred to as pEGFP-H5 [Appendix 3].

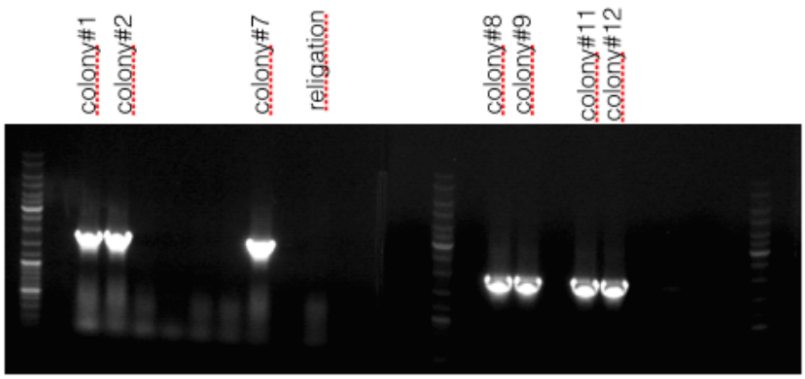

Figure 5.10. Cloning of H5 into pEGFP vector and colony PCR for selection of positive colonies. 7 out of 16 colonies gave band in the correct size, and they sent for sequencing. Colony#8's sequence was confirmed to be used in the upcoming experiments.

5.5.2. Co-transfection of HEK293T cells with pEGFP-H5 and pmCherry-ASC & confocal analysis

EGFP-H5 is a fusion protein encoded by the commercial plasmid pEGFP (Clontech, USA). H5 refers to the 565 amino acids long peptide encoded by the multiple cloning site at the C-terminus of the EGFP. When the plasmid expressing EGFP-

H5 is co-transfected with the plasmid expressing mCherry labelled ASC (by Ali Can Sahillioğlu) into HEK293T cell line, it is clearly shown that there is a perfect co-localization of H5 protein on ASC speck [Figure 5.11,Figure 5.12,Figure 5.13]. Whereas, no co-localization observed when mCherry-ASC and only EGFP expressing plasmids were co-expressed. 95% cells expressing EGFP-H5 and mCherry-ASC together was shown to aggregate the H5 proteins on ASC specks. Results are representative of three independent experiments.

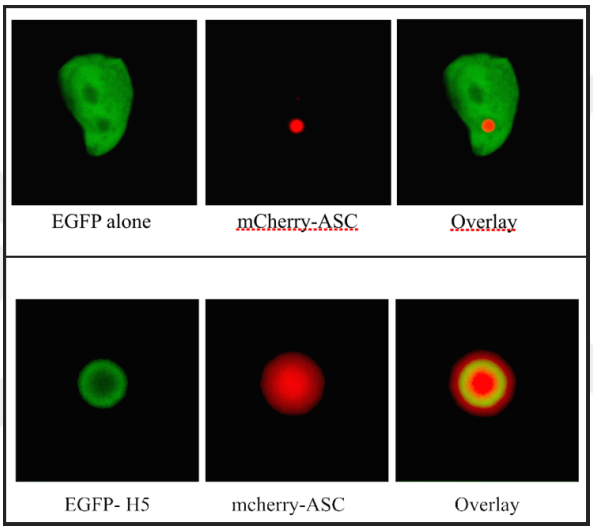

Figure 5.11. The co-aggregation of EGFP fluorescently labelled H5 on the mCherry-ASC speck.

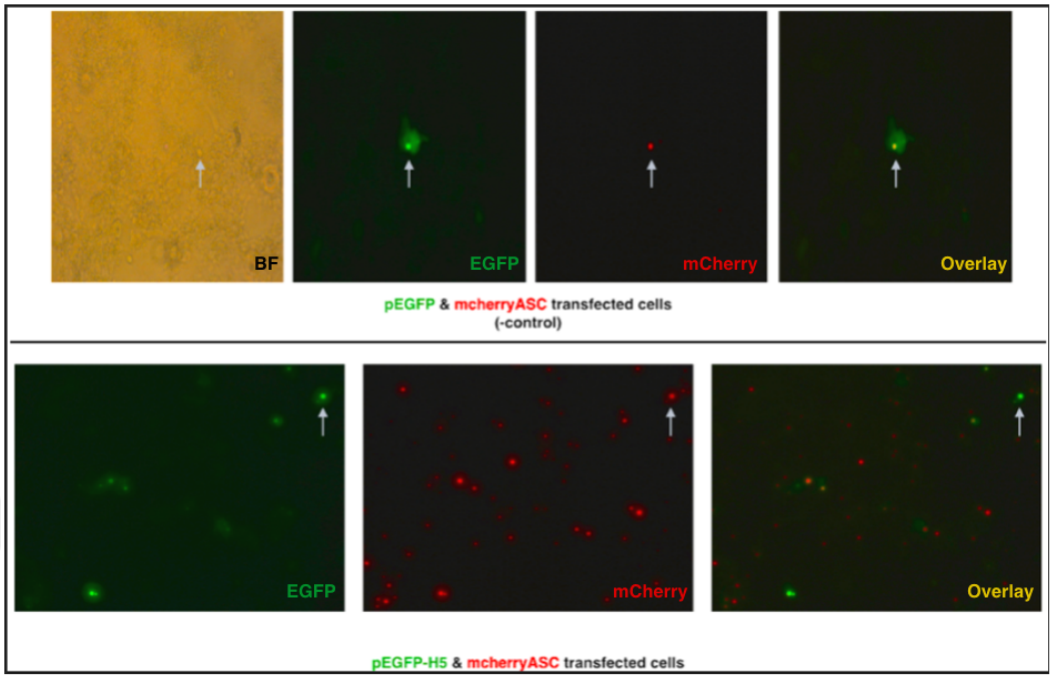

Figure 5.12. The co-aggregation of EGFP fluorescently labelled H5 on the mCherry-ASC speck observed with fluorescent microscopy.

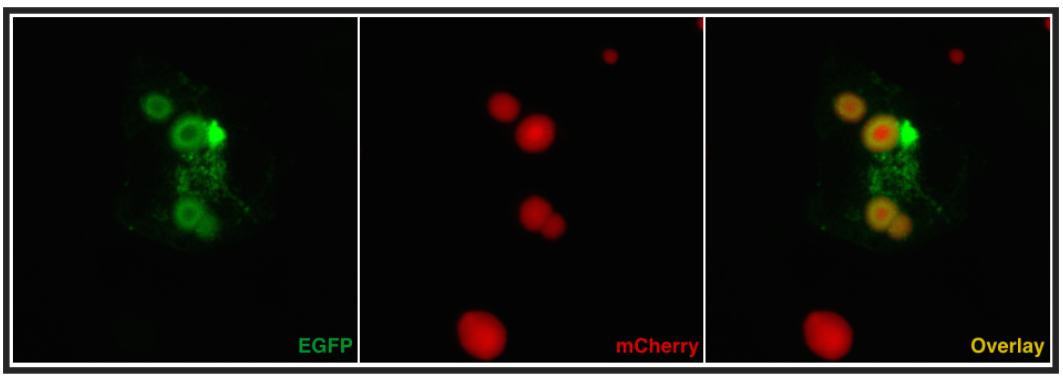

Figure 5.13. The co-aggregation of EGFP fluorescently labelled H5 on the mCherry-ASC speck observed with confocal microscopy.

It is clearly shown that full lenght H5 can co-aggregate on ASC specks if present in the same cell.

5.6. Generation of H5 loaded ASC specks

For immunization studies, we needed to produce H5-ASC fusion proteins. Otherwise we would not be able to determine the ratio of H5 co-aggregated on ASC protein. This would make problems when we want to determine the optimum/safe concentration of the vaccine for mice injections. Thus, we cloned full lenght H5 fused to N-terminus of ASC.

5.6.1. Cloning of H5 into pcDNA3-hASC vector

H5 (1695 bp) was amplified with Q5 DNA Polymerase by using designed primers from H5 containing pBS SK(+) vector (Addgene). Both the plasmid and the insert were digested with HindIII restriction enzyme. Ligation products were transformed into Stable3 competent bacteria. Positive colonies were detected with CMV-F and H5-R primers in colony PCR [Figure 5.14]. This construct is referred to as pcDNA3-H5-ASC [Appendix 1].

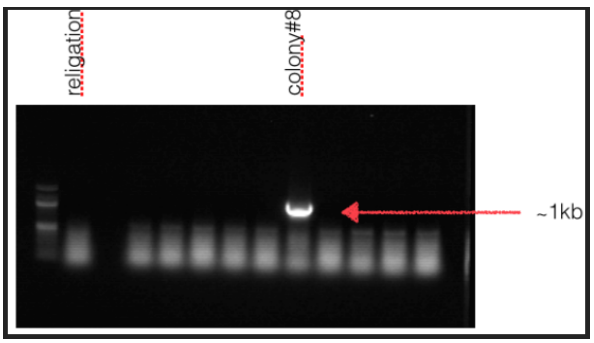

Figure 5.14. Cloning of H5 into pcDNA3-hASC vector and colony PCR for selection of positive colonies. 1 colony out of 10 gave the correct band in colony PCR. Colony#8's sequence is confirmed.

We attempted purification of full lenght H5 loaded ASC specks from HEK293T cells. Since we observed low production of H5-ASC protein, we did another cloning. The cause of this low expression could be because of the size of full lenght H5 and this

may prevent its accumulation on ASC, or may prevent the fusion proteins' folding. So, the most antigenic part of H5N1 *H.Influenza* virus, aminoacids from 69 to 133 [37], were fused to ASC's N-terminus [Figure 5.15].

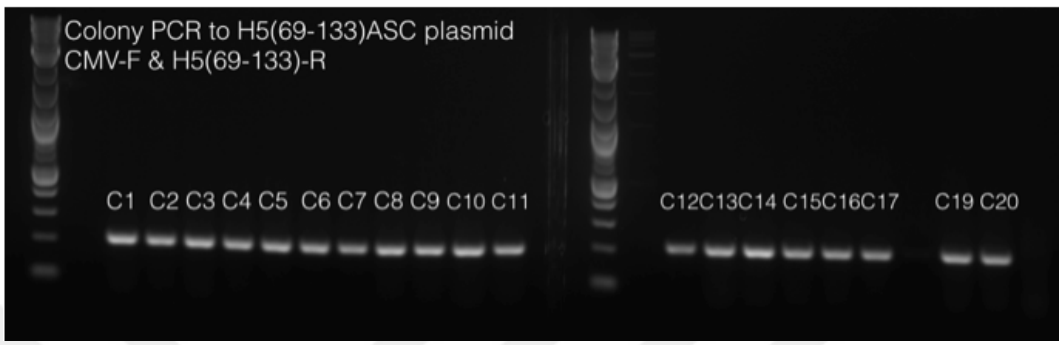

Figure 5.15. Cloning of H5(69-133) into pcDNA3-hASC vector and colony PCR for selection of positive colonies. 20 out of 21 picked colonies gave the correct band in colony PCR and colony#10's sequence is confirmed to be used in the experiments.

5.6.2. H5-ASC fusion protein production and purification

After transfection of pcDNA3-H5(69-133)-ASC plasmid into HEK293T cell line we were able to achieve good production of specks and we performed ASC speck purification till we obtained sufficient protein for mice injections.

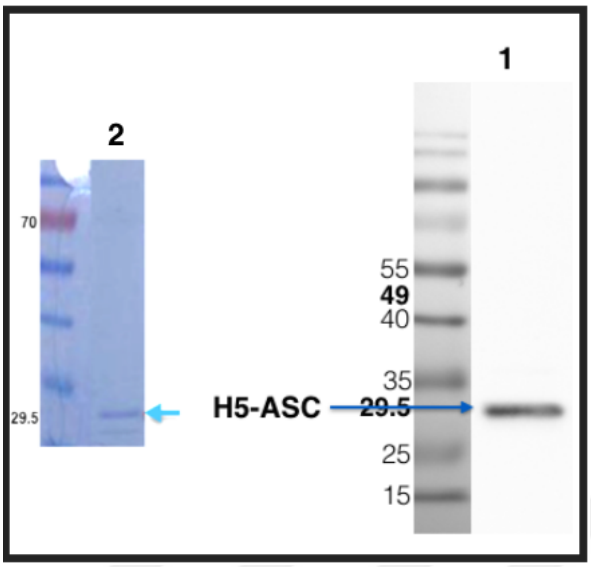

Figure 5.16. Purified H5-ASC specks from HEK293T cell line. A) Lane 1 represents the western blotting for H5(69-133)-ASC speck, done with anti-ASC antibody. B) Lane 2 demonstrates the purified H5(69-133)ASC specks with coomassie staining for concentration observation.

5.7. H5 protein production for immunization experiments as a control group.

Due to the high price of commercial H5 protein, we aimed to produce the protein for our planned functional experiments.

5.7.1. Cloning of H5 into pET30a(+) vector

H5 (1695 bp) was amplified with Q5 DNA Polymerase by using designed primers from H5 containing pBSSK vector. Both the plasmid (pET30a(+)) and the insert were digested with HindIII restriction enzyme. Ligation products were transformed into Stable3 competent E.coli bacteria. Positive colonies were detected with T7-F and H5-R primers in a colony PCR set up [Figure 5.17]. This construct is referred to as pET30a-H5 [Appendix 2]. Since we want to produce the H5 protein from the bacterial

culture, bacterial expression vector pET30(a) was preferably chosen.

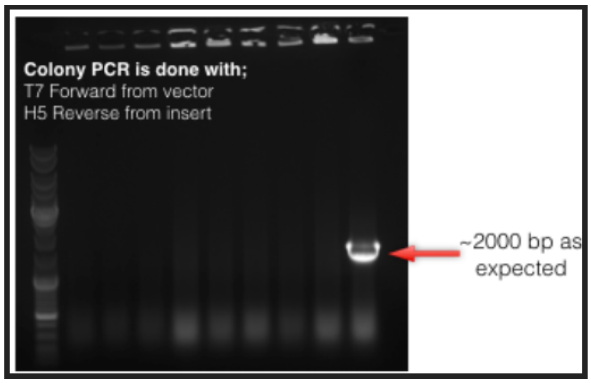

Figure 5.17. Cloning of H5 into pet30a+ vector and colony PCR for selection of positive colonies. First lane was the negative control with religation. 1 out of 7 colonies gave correct band in colony PCR and its sequence correction is verified.

5.7.2. IPTG induced H5 expression and purification

Another advantage of pET30(a) vector is its ability to code for the histidine protein. After we achieved cloning of H5 part of H5N1 into His tag containing pet30a+ (bacterial inducible expression vector), we produced His tagged H5 protein from bacterial culture by IPTG induction [Figure 5.18]. Histidine tag enabled us to purify H5 from the culture. In order to purify the protein from the culture, we used His-Trap column purification kit (GE Helathcare). These columns have nickel coupled to the chelating matrix of the columns. Tagging proteins with additional histidines, like (His)6, increased the affinity for Ni2+ and made the His-tagged protein the strongest binder among other proteins in the E. coli extract. Purified H5 was detected via Commassie staining [Figure 5.19].

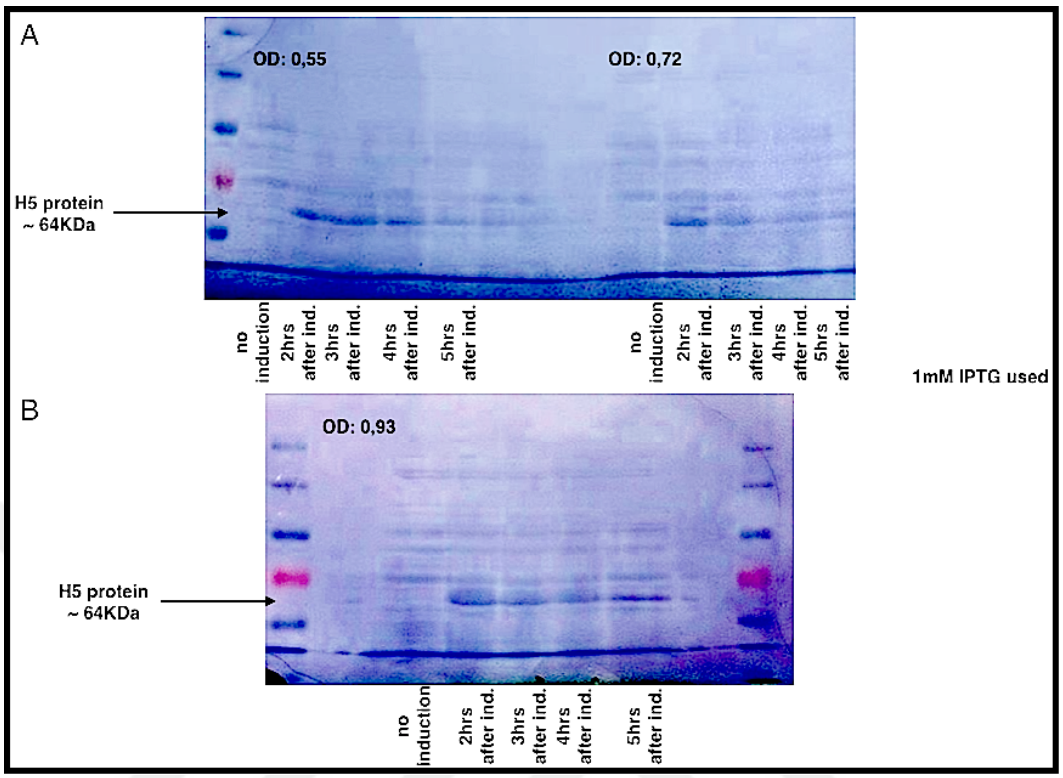

Figure 5.18. H5 protein production from bacterial culture. A,B) IPTG induction optimization.

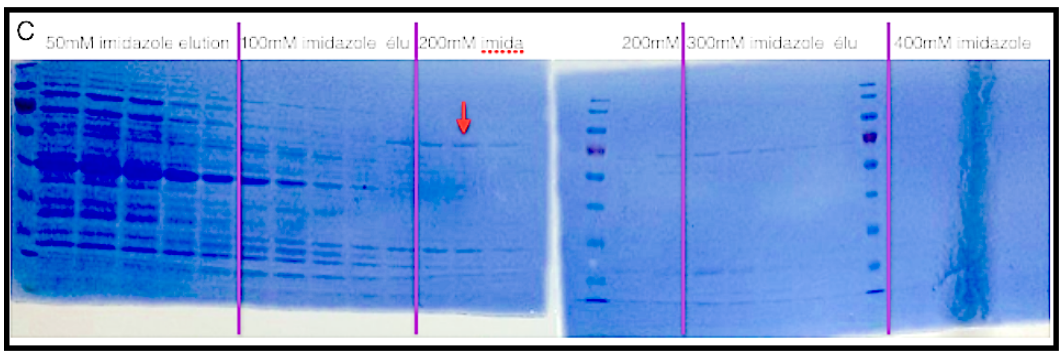

Figure 5.19. H5 protein purification from bacterial culture. C) Purification of H5, elution done at optimum (200mM) imidazole concentration.

5.8. Detection of H5 specific humoral immune responces

After we demonstrated the competency of OVA-ASC fusion speck immunization, we wanted to detect the humoral immune response of H5-ASC fusion speck immunizations. 50μg H5 loaded ASC specks injections were done to 4 C57/BL6 mice per sample. H5-ASC fusion protein, H5-Freund's adjuvant mixture, H5 protein were done 3 times with 2 week intervals. (Freund's adjuvant is used as a positive control, only antigen injections are used as a negative control.)

Injection of H5-ASC fusion specks increased the H5 specific IgG production with respect to control groups when we compared OD values [Figure 5.20]. Concentration calculation must be done with the standarts in order to observe the significancy of this experiment. More specific H5 antibody must be used to be sure about the standarts. Also, commercial pure H5 protein must be taken, as H5 protein used in this study may contain bacterial impurities which negatively effects our results.

In these experiments the total amount of injected protein was kept constant at 50μg. However, it should be noted that 50μg H5-ASC fusion protein contains 1/3 amino acids of H5 & 2/3 ASC. Thus, the H5 antigen is 2/3 less than the pure H5-Freund's complex condition.

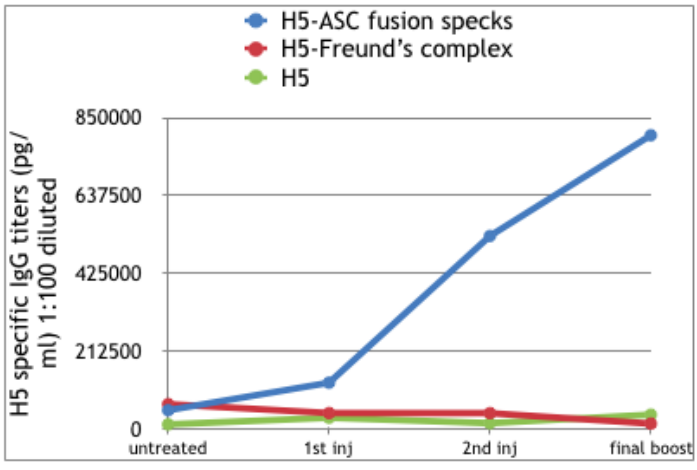

Figure 5.20. H5-ASC i.p. injection promoted H5 specific IgG production.

5.9. Antitumor activities of OVA loaded ASC specks.

Many studies are conducted for suppression of tumor growth using the EG.7/EL4 murine lymphoma model. Therefore, we designed an experiment to check antitumor activity of ASC specks by vaccinating C57BL/6 mice bearing ovalbumin (OVA)–expressing EG.7 thymoma tumors with the model tumor antigen (OVA) loaded ASC specks.

We injected $2,5 \times 10^6$ EG.7/EL4 (OVA) cells to the right flank of 6 mice. Only 2 of them developed tumor. When the tumor size become palpable, we did 50μg i.p. OVA-ASC injections 3 times with 1 week intervals. We observed that after the first injection tumor size doubled [V=1875 mm3]. When the second injection was done, the tumor size drastically fell by half [V=650mm3]. Size was steady till day 30, but within one day the size sharply increased by five-fold [V=5000mm3] [Figure 5.21 A)].

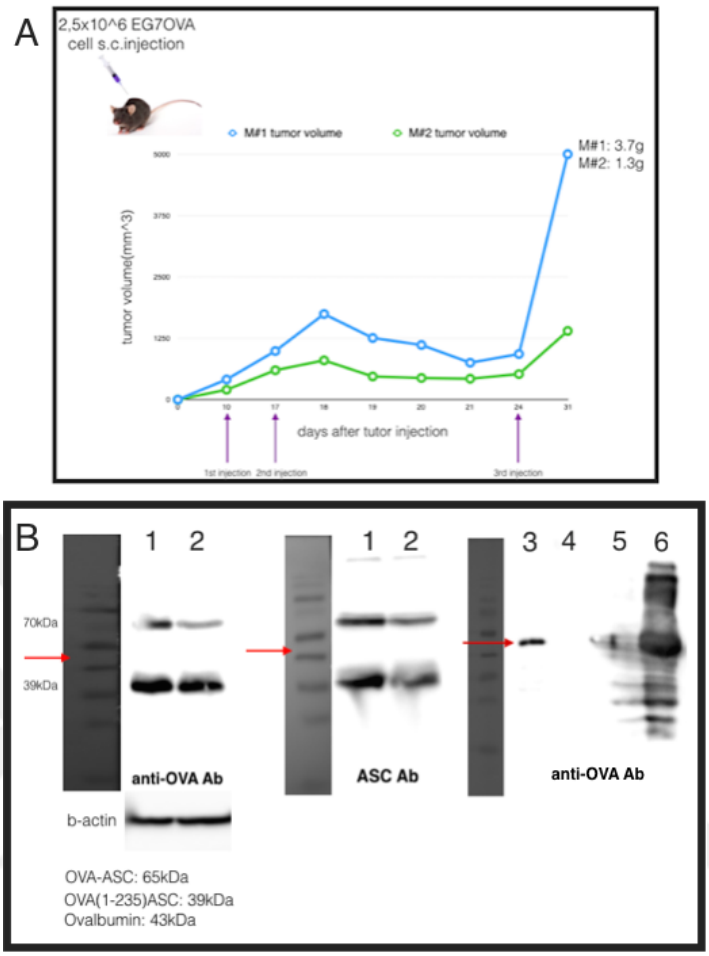

Figure 5.21. A)Change in tumor size upon OVA-ASC i.p. injections. $2,5 \times 10^6$ EG.7 OVA cells injected. after the second OVA-ASC fusion speck i.p. injection, the tumor size decreased by half B)Western blot analysis of ovalbumin and ASC expression in tumor cell lysate. Lane 1 and 2 indicates the tumor from the 1st mouse, 2nd mouse respectively. Lane 3 is G418 treated EG.7OVA cell line. Lane 4 is non-G418 treated cell line. Lane 5 and 6 are the commercial ovalbumin in increasing concentrations (6ng, 60ng). Same bands observed in the tumor lysates after anti-OVA and anti-ASC antibody incubations.

It is known that (OVA)–expressing EG.7 thymoma cell line must be treated with G418 antibiotic every month. E.G7-OVA cells are G418-resistant and they are stably expressing 43 kDa ovalbumin if they are treated with G418 once a month. In our

experiment, we injected $2,5 \times 10^6$ EG.7-OVA cell subcutaneously to right flank of mice. We did not treat the mice with G418. Thus, we hypothesized that the sharp increment in tumor size may be because of the loss of ovalbumin secretion. We dissected the tumors and did western blotting to check the presence of ovalbumin expression in the tumor. We demonstrated that the 43kDa ovalbumin was not present in the tumor. Interestingly, i.p. injected OVA-ASC specks, which are composed of 65kDa OVA-ASC and 39kDa OVA-ASC (1-235 aminoacid deletion), were found in the tumor enviroment [Figure 5.21 B)].

These results indicate that OVA-ASC fusion specks have potential anti-tumor activity while the antigen OVA is expressed in the cells.

6. DISCUSSION

In its initial discovery the ASC protein was shown to have a unique nature of forming micrometer size specks. Then, it was found that ASC works as an adaptor protein in different inflammasome pathways. Following studies showed that caspase-1 dependent cytokine processing happens through ASC specks formation. It is called "speck" since ASC proteins aggregate together to form a micrometer size compact shaped speck like structure. Also, ASC specks have similarities with other aggresome-like structures. The most important difference of ASC specks from aggresomes are the rapid formation kinetics, which takes only few minutes. Highly specific PYD-PYD (pyrin domain) and CARD-CARD (caspase recruitment domain) interactions are thought to provide its rapid aggregation making it possible to form only one ASC speck per cell. It is reasonable that ASC speck forms in a rapid fashion in order to make quick immune response as it is in NF-κB pathway which is the first line of the protection.

It was previously reported that the ASC protein has important roles in antigen presentation via inflammasome dependent and independent mechanisms. Especially, the mechanism of the mostly used adjuvant "alum" depends on the ASC adaptor protein in the NLRP3 inflammasome pathway. In addition to this, it is known that there are health concerns about alum usage as an adjuvant in vaccines. Because of such safety concerns, there is an ongoing research to find new adjuvants for vaccine technology.

Since ASC specks have unique properties different from other aggresome-like structures, ASC may have advantageous aspects over them. Studies done in our laboratory have previously shown that cytoplasmic proteins can co-aggregate on ASC specks in HEK293T cells [PCT IB2012/053079]. This observation lead to an idea that cytosolic proteins originating from pathogens may also co-aggregate on ASC specks during intracellular infection, which makes the ASC speck a new instrument in antigen presentation. To check this hypothesis, preliminary studies in our laboratory have shown

that this aggregate is stable at 37°C over prolonged incubations; can be artificially loaded with the model antigen ovalbumin; can be purified; engulfed by macrophages (PMA differentiation on THP-1 cells) and localized in an acidic organelle upon engulfment, all of are important in antigen presentation. In the last two years, other research groups supported our findings by demonstrating in *in vivo* studies that extracellular ASC specks are engulfed by other macrophages upon infection and those macrophages are activated and formed their own specks [18, 19]. We did experiments to support our initial hypothesis more and have done *in vivo* studies with mice to show antigen delivery and adjuvant ability of ASC specks.

Currently studies are conducted to develop particulate adjuvants which can target APCs and preferably after a single injection activate immunity for sufficient antibody production against the pathogen. Macrophages and dendritic cells are the most important APC types in the immune system. Thus, we wanted to demonstrate that ASC specks can be engulfed by BMDCs as it was previously shown for macrophages in our laboratory. Although it was difficult to work with dendritic cells for confocal analysis, since they are unattached cells, we clearly showed that they engulf OVA loaded ASC specks. We had to fix the cells on the slide, otherwise we could not focus on the cell. This drawback prevented us from tracking the degradation of ASC specks inside the cell.

Our initial aim was to load ASC specks with a known antigen H5 (the coat protein of *H.Influenza* virus). We have chosen H5, as viral infections trigger NLRP3 and AIM2 inflammasome pathways which are followed by ASC speck formation. Also, the presence of the influenza nucleoprotein at DALIS has been shown in DCs before [38] and it has been shown that cytosolic DNA co-localizes with the ASC speck upon stimulation of the AIM2 inflammasome [39]. So, it would be interesting to show influenza H5 protein's co-aggregation on the ASC speck. Our results demonstrate that H5 co-aggregates onto ASC speck upon co-transfection of pmCherry-ASC fusion protein with pEGFP-H5 construct into HEK293T cells. Later, the same experiment was repeated 3 times and gave the same results, confirming that we can use the ASC speck as a novel antigen delivery system as a prototype vaccine for H5N1 influenza.

When the H5-ASC fusion protein expression was performed in HEK293T cells, we found that H5-ASC can be produced and purified in sufficient quantities for *in vivo* studies. As a next step, we have done mice immunization studies with the produced fusion constructs and proteins to evaluate the full potential of ASC specks for vaccination applications. First and foremost we started with mCherry-ASC i.p., i.v., s.c. injections to show the safety, stability, route of ASC speck when injected into the mice body. IVIS Spectrum *in vivo* imaging system provided us to track the specks. We demonstrated that ASC specks are stable up to 3 weeks inside the mouse body and they are degraded afterwords. Both i.p. and i.v. injected specks localize to the spleen which is an important immune organ, especially for immunization to promote T&B cell populations which then lead to antibody production and immune memory. Although we have done this experiment with 50μg mCherry-ASC specks injections, there was no clogging of the blood vessel after i.v. injection and no any other extreme activation of the immune system to result in death of the mice or overt health effects. These results support ASC specks' safety further.

After we observing the safety of ASC speck injections, we started immunization experiments to compare antigen specific IgG titers to show the competency of our purposed antigen delivery system to generate antigen specific responses. We used Freund's adjuvant (*Mycobacterium tuberculosis* extract emulsified in mineral oil and used to boost immunity) as a positive control. Antigen itself was used as a negative control. In OVA-ASC, OVA-Freund's, OVA-PBS injection set, we saw high immune response in Freund's adjuvanted group of mice as expected. OVA itself did not alter the IgG levels as would be hoped. Our expectation was to see a significant increase in OVA-ASC vaccinated mice IgG titers, and indeed it made a significant increase. It was not as much as in OVA-Freund's mice sera, but it is normal. Since, Freund's adjuvant is known to be the best booster of immunity. Also, the ovalbumin amount in OVA-Freund's was 50 μg while the ovalbumin amount was 25 μg in 50 μg injected OVA-ASC vaccine. So, we conclude that our hypothesis about ASC speck for its antigen delivery and adjuvant ability is verified. In H5-ASC, H5-Freund's, H5-PBS injection set, we saw immune response in H5-ASC fusion speck injected mice group. Since there was an unexpected problem with the standarts we could not calculate the concentration of

IgG produced against H5 protein to give the significancy of this test. Yet, it was clearly shown that H5-ASC boosted immunity and promoted antibody production against H5 antigen when compared to negative control. Yet, we must repeat the experiment with a specific antibody against H5 in order to be sure about the standarts for concentration calculations. Also, we must buy commercial pure H5 protein in order be sure about the purity of H5 to be used as a negative control.

If T lymphocytes receives a co-stimulation signal or their receptors bind to a presented antigen, thymus originated T lymphocytes will mature in the periphery and become activated in the spleen/nodes. CD4+ T cells differentiate and start to secrete IL-2, IFN-γ and TNF-β for viral clearance by supporting T cells and macrophages, and IL-4, IL-6, IL-6, IL-10, IL-13 for parasitic clearance by supporting B lymphocytes. If surface immunoglobulins of B lymphocytes bind to an antigen, bone marrow originated B lymphocytes will be mature in secondary lymphoid tissues and become activated in the spleen/nodes. Then, they will differentiate either in antibody secreting cells (plasma cells) or in memory B cells [10]. Thus, we wanted to examine B&T cell populations in the immunized mice spleens upon vaccination. We demonstrated that OVA-ASC fusion protein injection decreased Mϕ population and increased CD4+T & B cell populations with respect to control groups. We suggested that the injected OVA-ASC specks are engulfed by Mϕ and lead to cytokine secretion followed by Mϕ burst and protein release to the extracellular matrix. Binding of BCR receptors of B cells to the molecules coming from Mϕ engulfed and loaded to the MHC-II receptors for full activation of B cells by CD4+T cells. Binding of CD4+T cells to MHC-II receptor of B cell will lead to interleukin secretion of Th2 cell to activate the B cell to proliferate.

The most commonly used vaccine adjuvants are alum (aluminium sulfate; for humans) and incomplete Freund's adjuvant (for animals). There is a need for better adjuvants for vaccines since they are not enough to induce effects with desired immunity. Thus, scientists are working to develop novel adjuvants for cancer immunotherapy [40]. In our study, we checked the anti-tumor vaccine activity of ASC specks in ovalbumin (OVA)–expressing EG.7 thymoma tumors. 2 out of 6 C57/BL6 mice developed OVA-secreting tumor on the right flank of C57/BL6 mice after subcutaneous

tumor injection. We did intraperitoneal OVA-ASC injection to educate macrophages against the ovalbumin antigen. Thus, our goal was to educate the immune system against OVA and promote the infiltration of educated immune cells into the tumor site, which then would lead to a decrease in tumor size. Our hypothesis was confirmed by demonstrating the 50% decrease in the tumor size after OVA-ASC i.p. injection. Yet, when we observed the sharp increase in the tumor size after 30 days, we thought it may be because of the lack of OVA expression in the tumor site. We checked the ovalbumin protein expression of the tumor and confirmed the ovalbumin loss. In order to be more accurate, ovalbumin expression of EG.7-OVA cell lysate before mice injection must be shown. What we have observed was interesting. Injected OVA-ASC is observed in western blotting result of the tumor lysate which suggests that the injected OVA-ASC is engulfed by antigen presenting cells (APCs) and infiltrate into the tumor site. This experiment must be repeated to compare the effect of OVA-ASC with negative control (OVA-PBS) and positive control (OVA-liposomes/lipofectamine) in order to conclude anti-tumor vaccine activity of the ASC speck.

Our immunization studies show that antigen delivery with ASC specks are able to boost immunity and provide antibody production against the antigen. Although we did not use any adjuvant with OVA loaded ASC specks, the antibody production against OVA antigen was sufficient to induce immune response compared to control groups. We have proven that ASC specks can be used as H5 antigen delivery vehicle against *H.Influenza* virus. Humoral immune responses against H5-ASC fusion specks also supports that ASC specks can be used as a novel carrier& adjuvant modality in vaccine technology. Naturally, the challenge experiments must be done with the pathogen after antigen-ASC immunization to evaluate initial efficacy of the purposed vaccine before large-scale field tests are conducted. In addition, the adjuvanticity of ASC specks are further supported by our tumor development experiment. We have shown that ASC treatment not only slow down the tumor development but also significantly decreased the tumor mass. It would be also interesting to see whether tumor formation can be done on mice after immunization with ASC specks. Yet, a comprehensive analysis of ASC specks in antigen presentation pathways are essential to use ASC specks as a completely novel & home- made therapeutic or prophylactic tool.

REFERENCES

1. Kenneth, M., J. C. A., T. Paul, W. Mark, M. Allan and W. C. T., *Janeway's immunobiology*, Garland science, 2012.

2. Sborgi, L., F. Ravotti, V. P. Dandey, M. S. Dick, A. Mazur, S. Reckel, M. Chami, S. Scherer, M. Huber, A. Böckmann, E. H. Egelman, H. Stahlberg, P. Broz, B. H. Meier and S. Hiller, "Structure and assembly of the mouse ASC inflammasome by combined NMR spectroscopy and cryo-electron microscopy", *Proceedings of the National Academy of Sciences*, Vol. 112, No. 43, pp. 13237–13242, 2015.

3. Takeuchi, O. and S. Akira, "Pattern Recognition Receptors and Inflammation", *Cell*, Vol. 140, No. 6, pp. 805–820, 2010.

4. Duthie, M. S., H. P. Windish, C. B. Fox and S. G. Reed, "Use of defined TLR ligands as adjuvants within human vaccines", *Immunological Reviews*, Vol. 239, No. 1, pp. 178–196, 2011.

5. Vajjhala, P. R., A. Lu, D. L. Brown, S. W. Pang, V. Sagulenko, D. P. Sester, S. O. Cridland, J. M. Hill, K. Schroder, J. L. Stow, H. Wu and K. J. Stacey, "The inflammasome adaptor ASC induces procaspase-8 death effector domain filaments", *Journal of Biological Chemistry*, Vol. 290, No. 49, pp. 29217–29230, 2015.

6. Mariathasan, S. and D. M. Monack, "Inflammasome adaptors and sensors: intracellular regulators of infection and inflammation", *Nat Rev Immunol*, Vol. 7, No. 1, pp. 31–40, 2007.

7. Yamazaki, T. and T. Ichinohe, "Inflammasomes in antiviral immunity: clues for influenza vaccine development.", *Clinical and experimental vaccine research*, Vol. 3, No. 1, pp. 5–11, 2014.

8. Bartl, S., M. Baish, I. L. Weissman and M. Diaz, "Did the molecules of adaptive

immunity evolve from the innate immune system?", *Integrative and comparative biology*, Vol. 43, No. 2, pp. 338–346, 2003.

9. Guo, X. and K. M. Dhodapkar, "Central and Overlapping Role Of Cathepsin B and Inflammasome Adaptor ASC In Antigen Presenting Function Of Human Dendritic Cells", *Human immunology*, Vol. 73, No. 9, pp. 871–878, sep 2012.

10. Siegrist, C.-a., "General aspects of vaccination", *Vaccine immunology*, Vol. 22, pp. 17–36, 2008.

11. Latz, E., T. S. Xiao and A. Stutz, "Activation and regulation of the inflammasomes", *Nat Rev Immunol*, Vol. 13, No. 6, pp. 397–411, 2013.

12. Fernandes-Alnemri, T. and E. S. Alnemri, "Chapter Thirteen Assembly, Purification, and Assay of the Activity of the ASC Pyroptosome", *Methods in Enzymology*, Vol. 442, No. 08, pp. 251–270, 2008.

13. Sahillioglu, A. C., F. Sumbul, N. Ozoren and T. Haliloglu, "Structural and dynamics aspects of ASC speck assembly", *Structure*, Vol. 22, No. 12, pp. 1722–1734, 2014.

14. de Alba, E., "Structure and interdomain dynamics of apoptosis-associated speck-like protein containing a CARD (ASC)", *Journal of Biological Chemistry*, Vol. 284, No. 47, pp. 32932–32941, 2009.

15. Sahillioglu, A. C. and N. Nozoren, "Artificial loading of ASC specks with cytosolic antigens", *PLoS ONE*, Vol. 10, No. 8, pp. 1–11, 2015.

16. Cassel, S. L. and F. S. Sutterwala, "Sterile inflammatory responses mediated by the NLRP3 inflammasome", *European journal of immunology*, Vol. 40, No. 3, pp. 607–611, mar 2010.

17. Fernandes-Alnemri, T., J. Wu, J.-W. Yu, P. Datta, B. Miller, W. Jankowski,

S. Rosenberg, J. Zhang and E. S. Alnemri, "The pyroptosome: a supramolecular assembly of ASC dimers mediating inflammatory cell death via caspase-1 activation", *Cell Death Differ*, Vol. 14, No. 9, pp. 1590–1604, jun 2007.

18. Franklin, B. S., L. Bossaller, D. De Nardo, J. M. Ratter, A. Stutz, G. Engels, C. Brenker, M. Nordhoff, S. R. Mirandola, A. Al-Amoudi, M. S. Mangan, S. Zimmer, B. G. Monks, M. Fricke, R. E. Schmidt, T. Espevik, B. Jones, A. G. Jarnicki, P. M. Hansbro, P. Busto, A. Marshak-Rothstein, S. Hornemann, A. Aguzzi, W. Kastenmuller and E. Latz, "The adaptor ASC has extracellular and 'prionoid' activities that propagate inflammation", *Nature Immunology*, Vol. 15, No. 8, pp. 727–737, 2014.

19. Sagoo, P., Z. Garcia, B. Breart, F. Lemaître, D. Michonneau, M. L. Albert, Y. Levy and P. Bousso, "In vivo imaging of inflammasome activation reveals a subcapsular macrophage burst response that mobilizes innate and adaptive immunity.", *Nature medicine*, Vol. 22, No. 1, pp. 64–71, 2016.

20. Baroja-Mazo, A., F. Martín-Sánchez, A. I. Gomez, C. M. Martínez, J. Amores-Iniesta, V. Compan, M. Barberà-Cremades, J. Yagüe, E. Ruiz-Ortiz, J. Antón, S. Buján, I. Couillin, D. Brough, J. I. Arostegui and P. Pelegrín, "The NLRP3 inflammasome is released as a particulate danger signal that amplifies the inflammatory response TL - 15", *Nature Immunology*, Vol. 15 VN - r, No. 8, pp. 738–748, 2014.

21. Whitehouse, C. A., S. Waters, K. Marchbank, A. Horner, N. W. A. Mcgowan, V. Jovanovic, G. M. Xavier, T. G. Kashima, M. T. Cobourne, G. O. Richards, P. T. Sharpe, M. Skerry, A. E. Grigoriadis and E. Solomon, "Correction for Whitehouse et al., Neighbor of Brca1 gene (Nbr1) functions as a negative regulator of postnatal osteoblastic bone formation and p38 MAPK activity", *Proceedings of the National Academy of Sciences*, Vol. 110, No. 11, pp. 4428–4428, 2013.

22. Lelouard, H., E. Gatti, F. Cappello, O. Gresser, V. Camosseto and P. Pierre, "Transient aggregation of ubiquitinated proteins during dendritic cell maturation",

Nature, Vol. 417, No. 6885, pp. 177–182, may 2002.

23. Andre, F. E., R. Booy, H. L. Bock, J. Clemens, S. K. Datta, T. J. John, B. W. Lee, S. Lolekha, H. Peltola, T. A. Ruff, M. Santosham and H. J. Schmitt, "Vaccination greatly reduces disease, disability, death and inequity worldwide", *Bulletin of the World Health Organization*, Vol. 86, No. 2, pp. 140–146, 2008.

24. Erdem, H. and M. Akova, "Leading infectious diseases problems in Turkey", *Clinical Microbiology and Infection*, Vol. 18, No. 11, pp. 1056 – 1067, 2012.

25. Garulli, B. and M. R. Castrucci, "Protective immunity to influenza: lessons from the virus for successful vaccine design", *Expert Rev Vaccines*, Vol. 8, No. 6, pp. 689–693, 2009.

26. Jefferson, T., C. Di Pietrantonj, L. A. Al-Ansary, E. Ferroni, S. Thorning and R. E. Thomas, "Vaccines for preventing influenza in the elderly.", *The Cochrane database of systematic reviews*, , No. 2, p. CD004876, jan 2010.

27. Osterholm, M. T., N. S. Kelley, A. Sommer and E. A. Belongia, "Efficacy and effectiveness of influenza vaccines: a systematic review and meta-analysis", *The Lancet Infectious Diseases*, Vol. 12, No. 1, pp. 36–44, aug 2016.

28. \spaceProgram\spaceSurveillance\spaceNetwork, T., "Evolution of H5N1 Avian Influenza Viruses in Asia", *Emerging Infectious Diseases*, Vol. 11, No. 10, p. 10, 2005.

29. WHO, "Options for the use of human H5N1 influenza vaccines and the WHO H5N1 vaccine stockpile", *World Health*, , No. October 2007, p. WHO/HSE/EPR/GIP/2008.1, 2007.

30. Russell, R. J., P. S. Kerry, D. J. Stevens, D. A. Steinhauer, S. R. Martin, S. J. Gamblin and J. J. Skehel, "Structure of influenza hemagglutinin in complex with an inhibitor of membrane fusion", *Proceedings of the National Academy of Sciences*

of the United States of America, Vol. 105, No. 46, pp. 17736–17741, nov 2008.

31. Gambaryan, A., A. Tuzikov, G. Pazynina, N. Bovin, A. Balish and A. Klimov, "Evolution of the receptor binding phenotype of influenza A (H5) viruses", *Virology*, Vol. 344, No. 2, pp. 432 – 438, 2006.

32. Baxter, D., "Active and passive immunity, vaccine types, excipients and licensing", *Occupational Medicine*, Vol. 57, No. 8, pp. 552–556, 2007.

33. O'Hagan, D. T., D. Rahman, J. P. McGee, H. Jeffery, M. C. Davies, P. Williams, S. S. Davis and S. J. Challacombe, "Biodegradable microparticles as controlled release antigen delivery systems.", *Immunology*, Vol. 73, No. 2, pp. 239–42, 1991.

34. Foged, C., B. Brodin, S. Frokjaer and A. Sundblad, "Particle size and surface charge affect particle uptake by human dendritic cells in an in vitro model", *International Journal of Pharmaceutics*, Vol. 298, No. 2, pp. 315–322, 2005.

35. Offit, P. a. and R. K. Jew, "Addressing parents' concerns: do vaccines contain harmful preservatives, adjuvants, additives, or residuals?", *Pediatrics*, Vol. 112, No. 6, pp. 1394–1397, 2003.

36. Tomljenovic, L. and C. A. Shaw, "Aluminum Vaccine Adjuvants: Are they Safe?", *Current Medicinal Chemistry*, Vol. 18, No. 17, pp. 2630–2637, 2011.

37. Li, J., Y. Wang, Y. Liang, B. Ni, Y. Wan, Z. Liao, K. H. Chan, K. Y. Yuen, X. Fu, X. Shang, S. Wang, D. Yi, B. Guo, B. Di, M. Wang, X. Che and Y. Wu, "Fine antigenic variation within H5N1 influenza virus hemagglutinin's antigenic sites defined by yeast cell surface display", *European Journal of Immunology*, Vol. 39, No. 12, pp. 3498–3510, 2009.

38. Herter, S., P. Osterloh, N. Hilf, G. Rechtsteiner, J. Hohfeld, H. G. Rammensee and H. Schild, "Dendritic cell aggresome-like-induced structure formation and delayed antigen presentation coincide in influenza virus-infected dendritic cells", *J*

Immunol, Vol. 175, No. 2, pp. 891–898, 2005.

39. Wu, J., T. Fernandes-Alnemri and E. S. Alnemri, "Involvement of the AIM2, NLRC4, and NLRP3 Inflammasomes in Caspase-1 Activation by Listeria monocytogenes", *Journal of Clinical Immunology*, Vol. 30, No. 5, pp. 693–702, 2010.

40. Temizoz, B., E. Kuroda and K. J. Ishii, "Vaccine adjuvants as potential cancer immunotherapeutics", *International Immunology*, 2016.

APPENDIX A: PLASMID MAPS

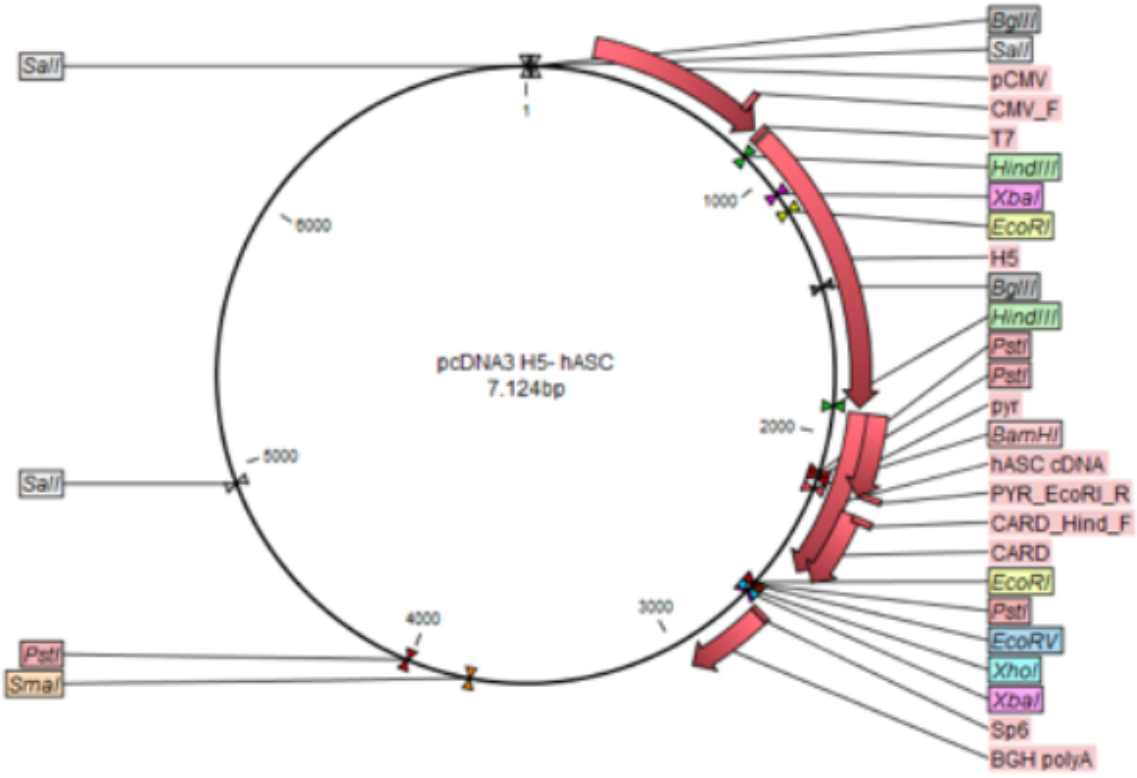

Figure A.1. Plasmid map of pcDNA3-H5-hASC.

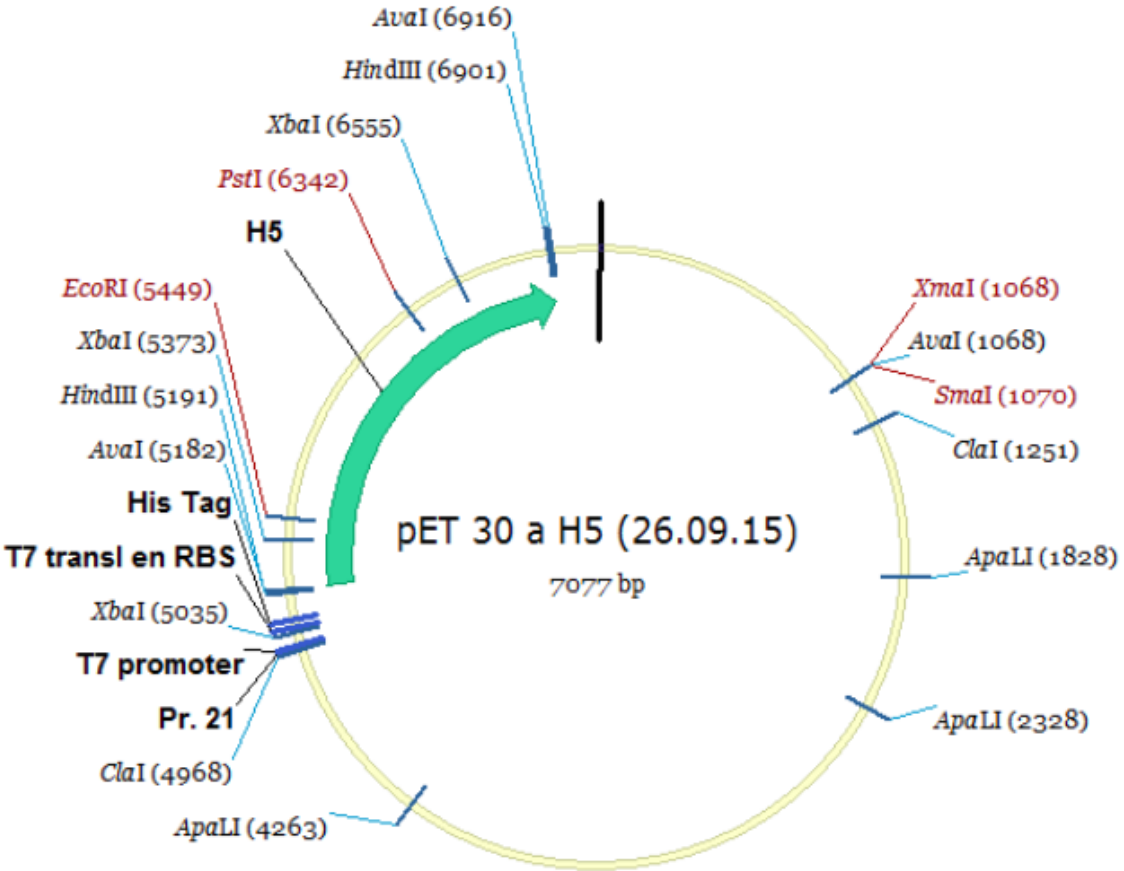

Figure A.2. Plasmid map of pet30a+H5.

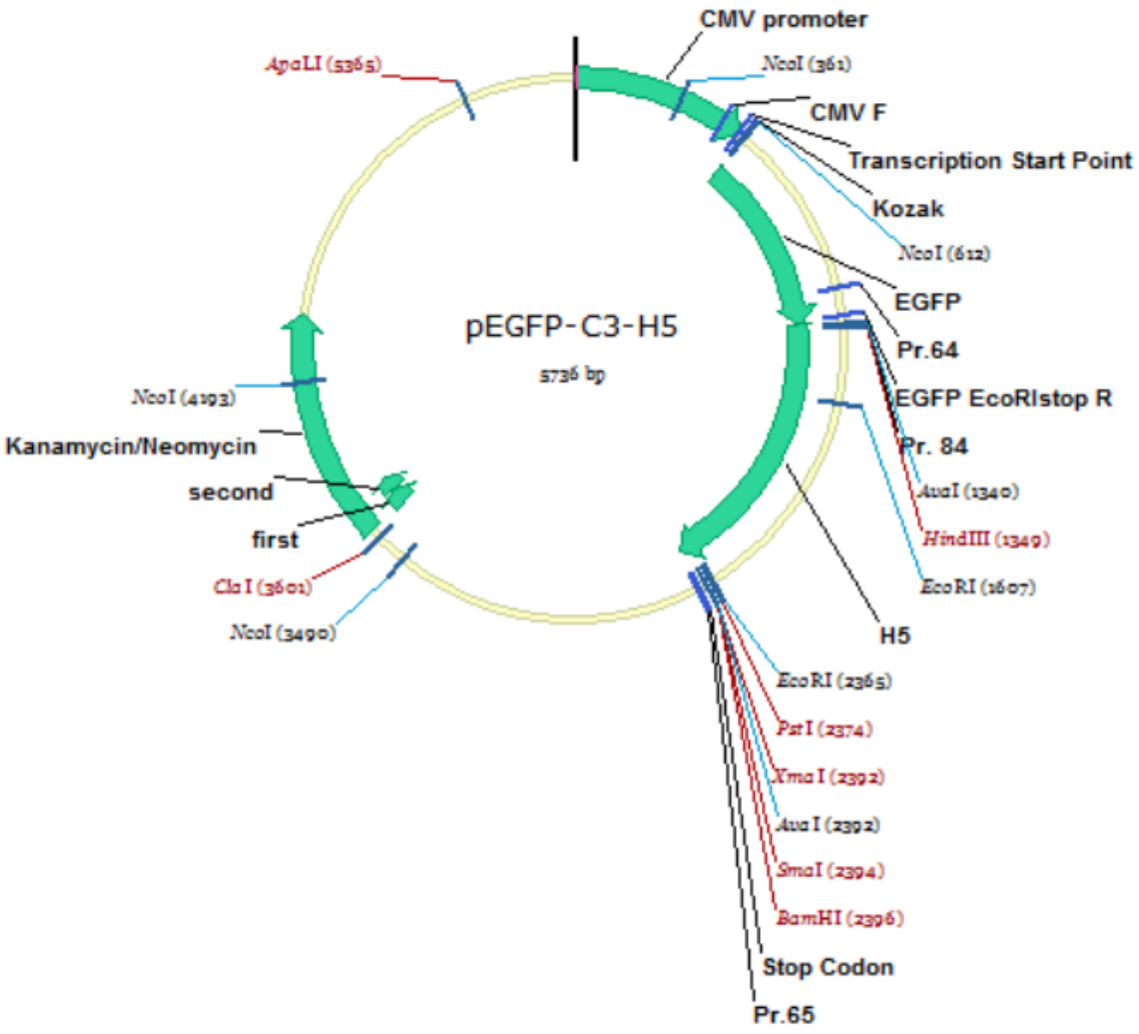

Figure A.3. Plasmid map of pEGFP-H5.

APPENDIX B: FACS ANALYSIS

Graphs of the analysed cells stained with different kind of cell surface markers can be found in the next pages.

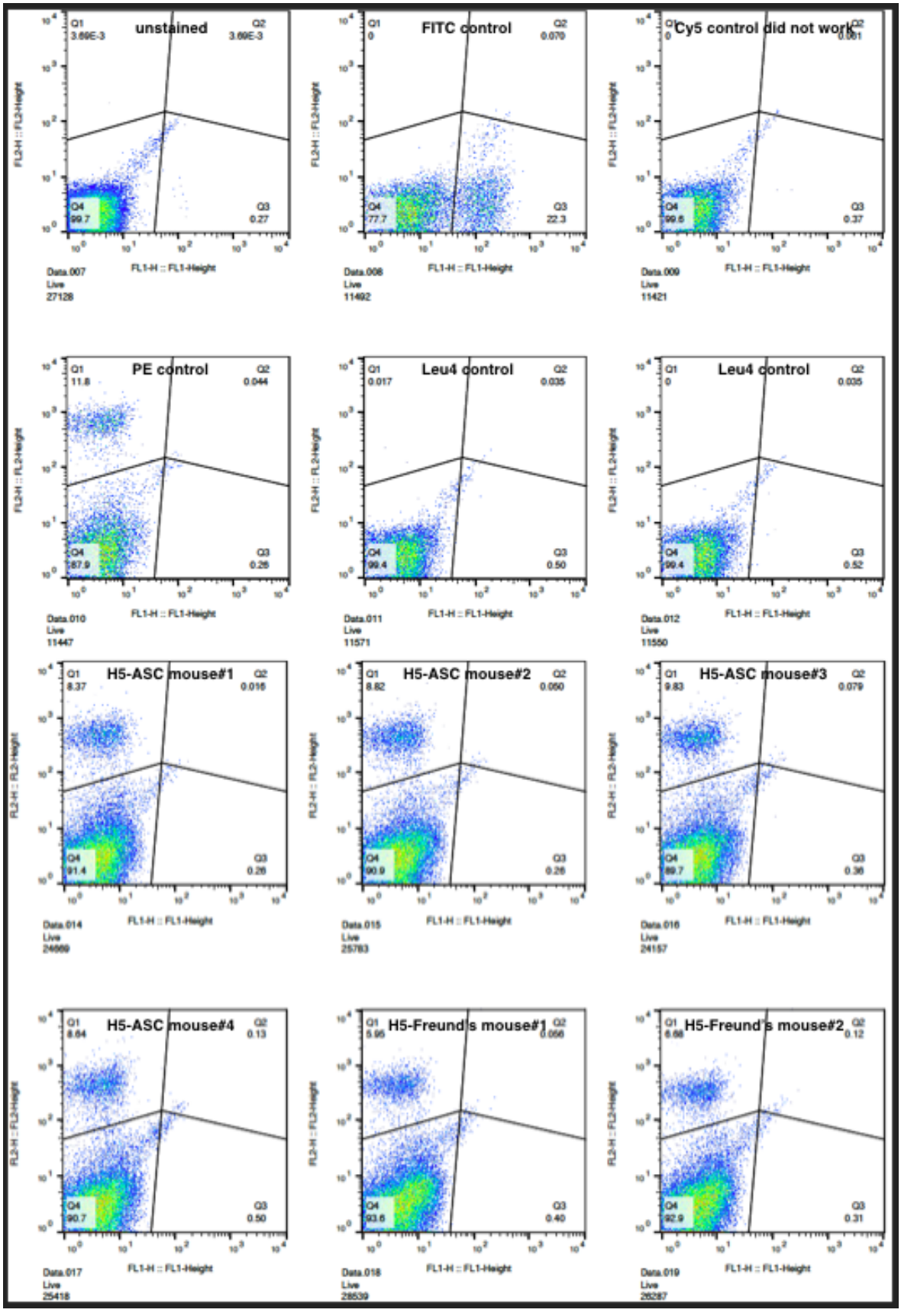

Figure B.1. Cells were stained for cell surface CD4, B220, H57 expression and assessed by flow cytometry.

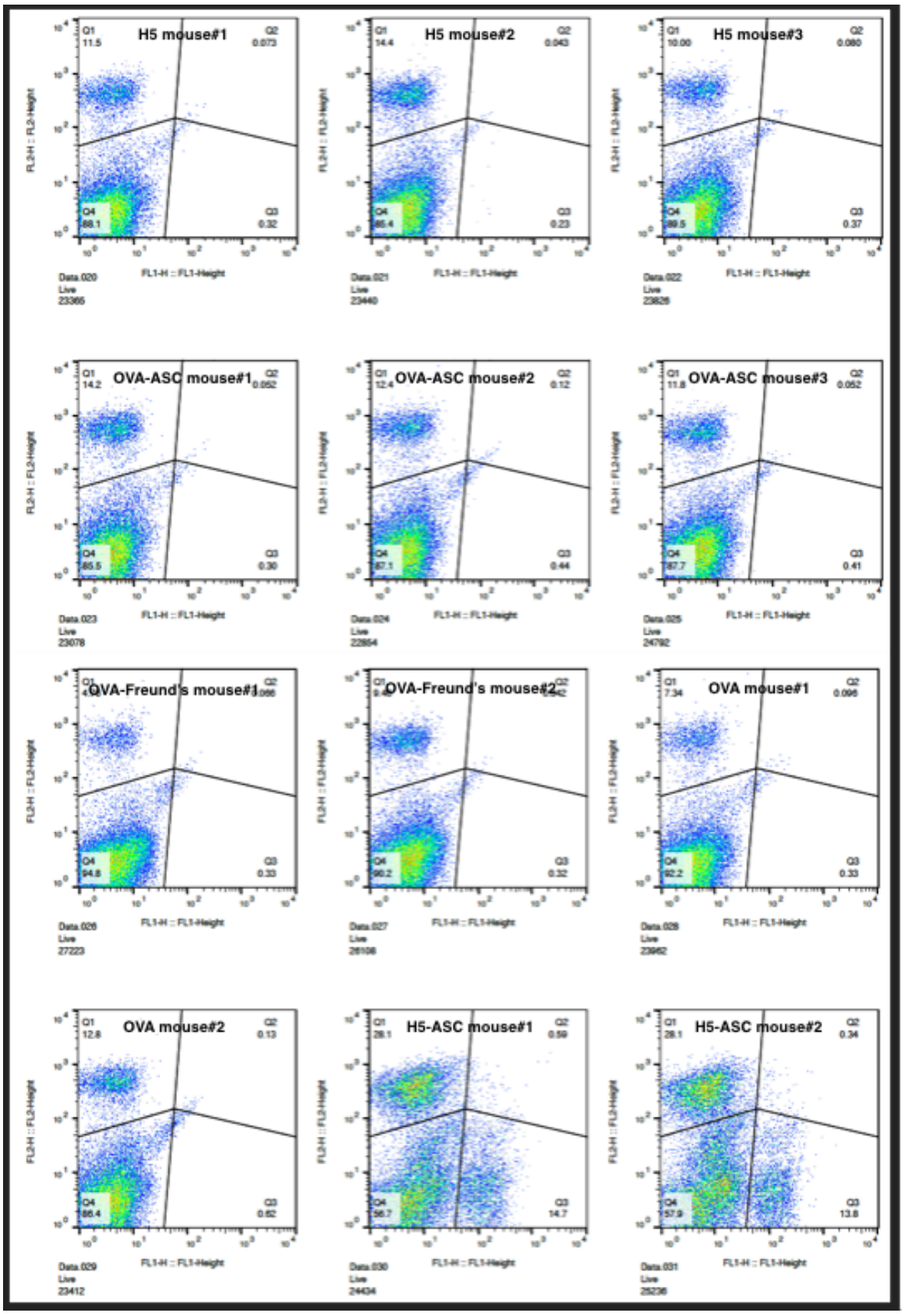

Figure B.2. Cells were stained for cell surface CD4, B220, H57 expression and assessed by flow cytometry.

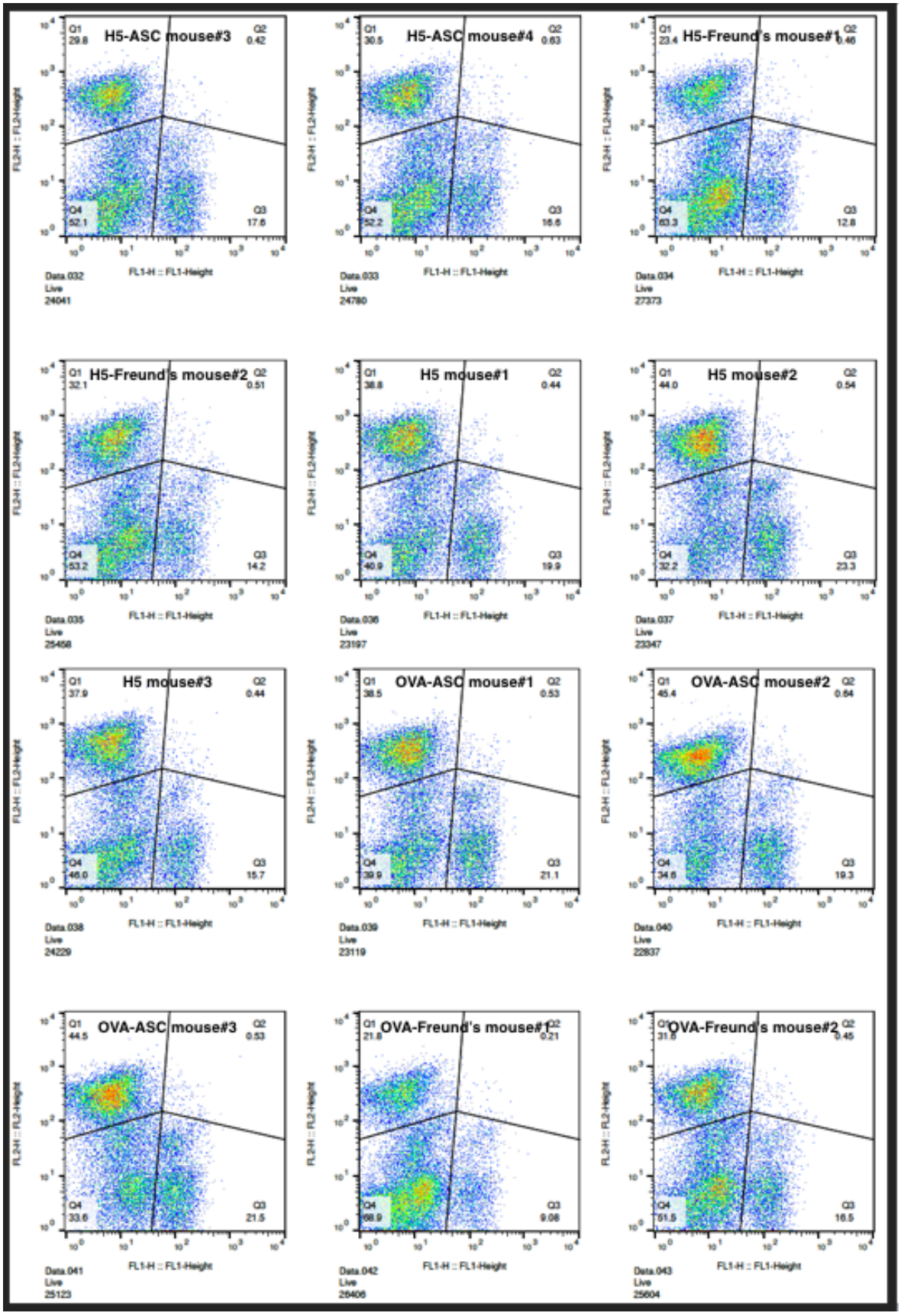

Figure B.3. Cells were stained for cell surface CD4, B220, H57 expression and assessed by flow cytometry.

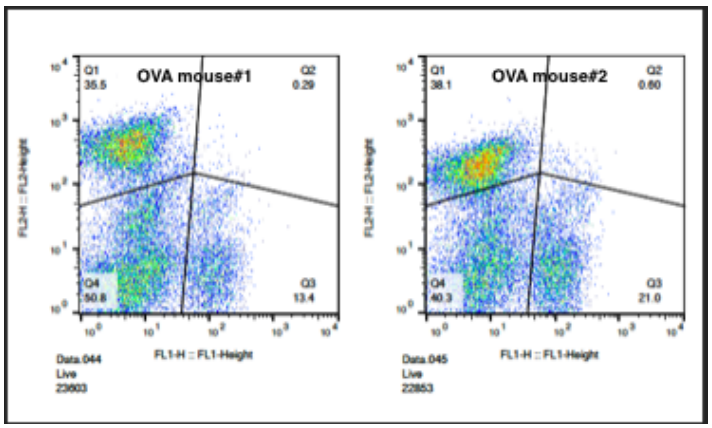

Figure B.4. Cells were stained for cell surface CD4, B220, H57 expression and assessed by flow cytometry.

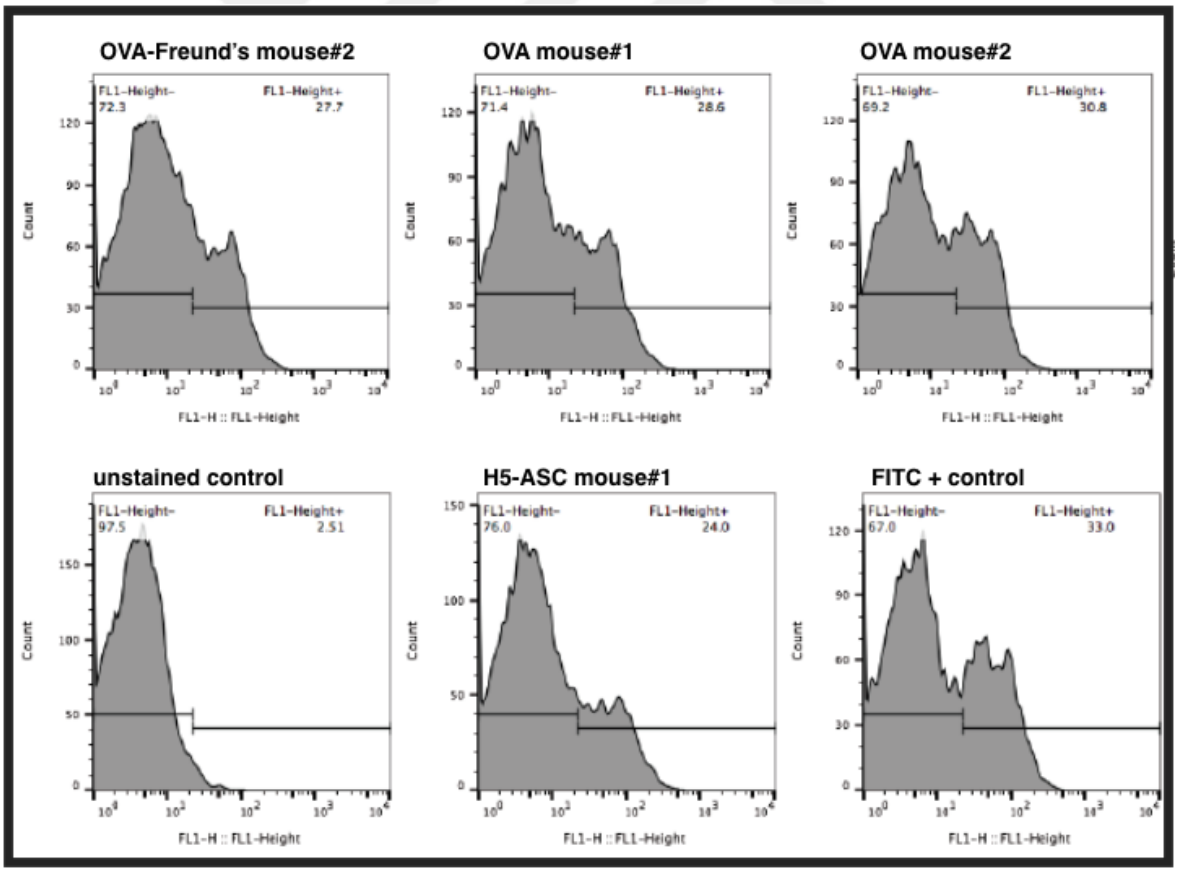

Figure B.5. Cells were stained for cell surface CD19 expression and assessed by flow cytometry.

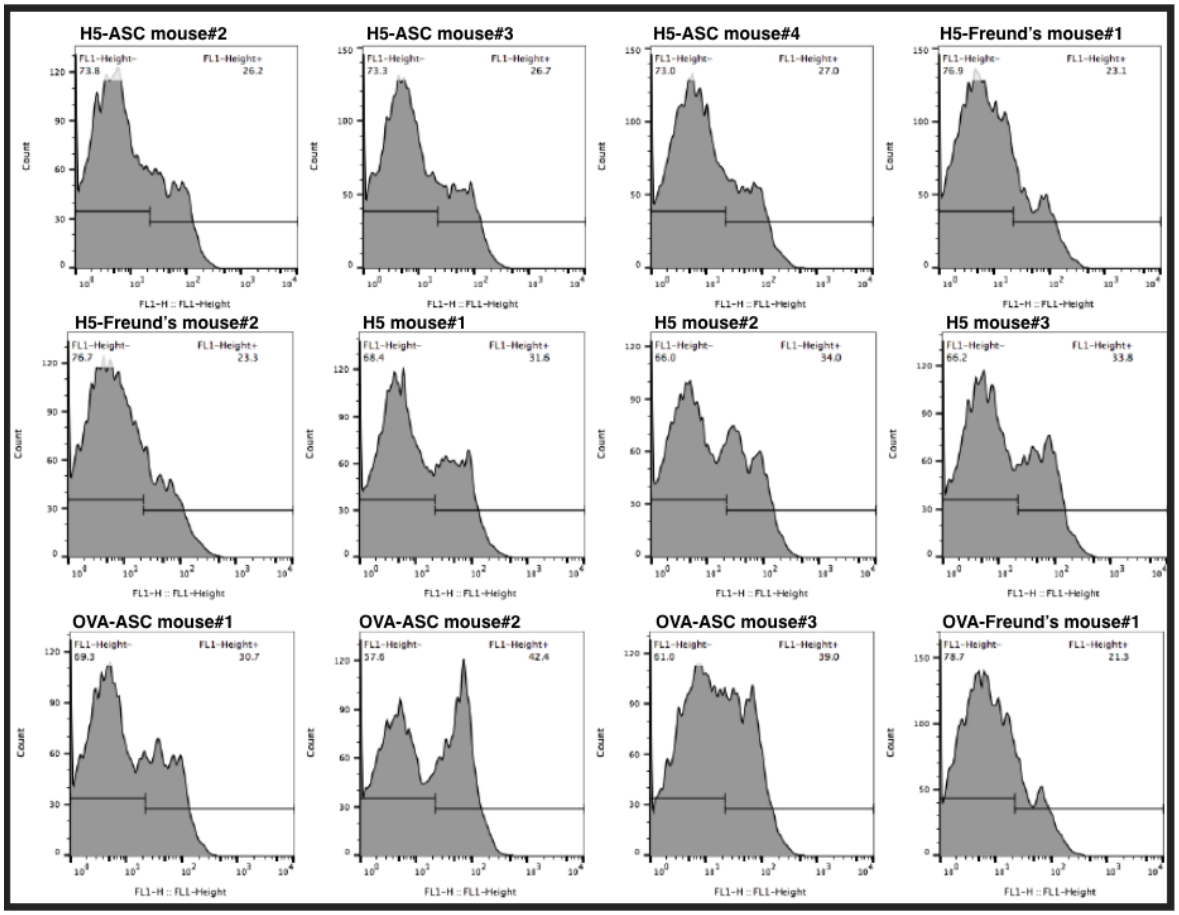

Figure B.6. Cells were stained for cell surface CD19 expression and assessed by flow cytometry.